

Contribution of surface bound positive charge towards the conversion of N-H to N-Cl on poly (ethylene terephthalate) and the antibacterial activity of the resulting N-Cl

by

Rajbir Kaur

A Thesis submitted to the Faculty of Graduate Studies of
The University of Manitoba
in partial fulfilment of the requirements of the degree of

MASTER OF SCIENCE

Department of Biosystems Engineering
University of Manitoba
Winnipeg

ABSTRACT

As a continued study on combined use of different antibacterial chemistries, *N*-chloramine and short chain Quaternary ammonium compound (QAC) were immobilized on modified poly (ethylene terephthalate) (PET) surface in various ratios via “click” chemistry. In this study, contribution of surface bound QAC to the conversion of cyclic and acyclic N-H to N-Cl, fastest recharging chlorination as well as the most effective antibacterial efficacy was investigated. Surface bound positive charge at the density of 8.4×10^{16} charges/cm² achieved highest equilibrium conversion and facilitated a nine-fold increase in conversion of sterically hindered acyclic N-H to N-Cl from 0.39 to 3.92%. Within the range of 2.8×10^{16} to 8.4×10^{16} charges/cm², highest active chlorine loading within first five minutes of chlorination was observed on sample loaded with 4.6×10^{16} charges/cm². As it comes to PET surface grafted with a cyclic *N*-chloramine precursor, the presence of 2×10^{16} charges/cm² enabled a five-fold increase in the conversion of cyclic N-H to N-Cl. The highest biocidal efficacy was observed for sample loaded with cyclic *N*-chloramine/QAC 17.2:10 which presented total kill of *E.coli* (5.8 log reduction) in 10 minutes compared to 1.9 log reduction for other ratios (22.8/10, 75.5/10) tested at a similar level of active chlorine (223±6ppm respectively).

ACKNOWLEDGEMENT

It is a privilege to express my deep sense of gratitude and indebtedness to Dr. Song Liu. It has been an honor and a great opportunity to work under his guidance. Dr. Song Liu has continuously helped me throughout my research study despite of his busy schedule and professional commitments. I appreciate his ideas, funding and time to make my research experience motivational and productive. I could not have imagined having a better mentor for my Masters study.

I would like to thank my committee members Dr. Martin King, and Dr. Stefan Cenkowski for their insightful comments which motivated me to widen my research from various perspectives.

I would like to express sincere thanks for the financial support from the Graduate Enhancement of Tri-Council Stipends (GETS), Special scholarship in textile science and International Graduate Student Scholarship (IGSS). I also want to thank my fellow labmates in Biomaterial Synthesis and Surface Engineering Lab and special thanks are extended to Mr. Sadegh Ghanbar for his suggestions and kind help for biocide synthesis. I acknowledge with thanks the help, inspiration and cheerful company of my friends Harjot Singh, Navriti Mittal, Seungil kim, Zahid Rahman, Sadigeh Nazaripour, Sogol Ashgari and Harshita Chaudhary. I fall short of words to describe the depth of gratitude towards my parents and siblings to whom I owe everything. Without their blessings this work could not have taken material form.

Last but not the least I thank the almighty for giving me strength to carry out my work with sincerity and honesty, and hope to carry this on in future.

TABLE OF CONTENTS

Abstract.....	0
Acknowledgement	1
Table of Contents.....	2
List of Tables	4
List of Figures	5
1 Introduction	6
1.1 Overview	6
1.2 Contact-active antibacterial agents	9
1.2.1 <i>N</i> -chloramines	9
1.2.1.1 Recharging Action	10
1.2.1.2 Conversion ratio of cyclic and acyclic N-H to N-Cl	12
1.2.1.3 Modification Techniques	14
1.2.2 Quaternary Ammonium Compounds.....	15
1.2.2.1 Effect of alkylation on antibacterial activity	15
1.2.2.2 Contact active QACs - Mechanism of action.....	17
1.2.2.3 Charge density threshold on surface for optimum antibacterial efficacy	19
1.2.2.4 Modification Techniques	21
1.3 Characterization study	22
1.3.1 Characterization of <i>N</i> -halamine	22
1.3.2 Characterization of QACs	23
1.3.2.1 Method to determine surface accessible quaternary amines	23
1.3.2.2 Zeta potential measurement	24
1.3.2.3 Reference data concerning positively charged surfaces.....	25
1.4 Combined action of <i>N</i> -chloramine and Quaternary ammonium compound	27
1.5 Gap in current Literature	28
1.6 Conclusion.....	29
2 Hypothesis and objectives	30

3	Experimental Design	32
3.1	Materials	32
3.2	Synthesis of monomer and biocides	33
3.2.1	Synthesis of N-(2-methylbut-3-yn-2-yl) acrylamide (MBAA)	33
3.2.2	Synthesis of <i>N</i> -chloramine precursor.....	33
3.2.3	Synthesis of Quaternary Ammonium Compound	35
3.3	Surface modification of PET: Semi-Interpenetrating Network	35
3.4	Surface modification of PET: Plasma technique	36
3.5	“Click” Reaction between PET-PMBAA or PET-PA and azido moieties.....	36
3.6	Chlorination and titration of active chlorine	39
3.7	Antibacterial Assessment of Modified PET	39
3.8	Zeta potential.....	40
3.9	Determination of positive charge on the surface of fabric.....	41
3.10	Removal of copper from clicked PET fabric	42
4	Results and Discussion	43
4.1	part 1: cyclic and acyclic N-H groups immobilized together on PET surface: a mixed system	43
4.1.1	Contribution of positive charge towards active chlorine loading.....	44
4.1.2	Contribution of positive charge towards Antibacterial efficacy	49
4.2	part 2: cyclic and acyclic N-H groups immobilized separately on pet surface.....	53
4.2.1	Methods to immobilize cyclic and acyclic <i>N</i> -H groups separately	53
4.2.2	Contribution of positive charge to chlorination of acyclic N-H groups.....	54
4.2.2.1	Titration of positive charge on PET-MBAA/QAS surface	56
4.2.2.2	Zeta potential values for PET-MBAA/QAS surface.....	58
4.2.2.3	Chlorination kinetics of PET-MBAA-QAS.....	61
4.2.3	Antibacterial efficacy of acyclic N-H groups in the presence of positive charge	68
4.2.4	Contribution of positive charge to the conversion of cyclic N-H groups	70
4.2.4.1	Titration of positive charge on PET-PA-AzH/QAS	73
4.2.5	Contribution of positive charge to antibacterial efficacy of cyclic N-H groups	74
5	Conclusions and future work	77
6	Reference list	82

LIST OF TABLES

Table 1-1 Initial deposition rate, percentages of growing bacteria of gram-positive and gram-negative bacteria on polymer films with varying charge density.....	25
Table 1-2 Characterization of QA-PEI nanoparticles at different degrees of alkylation.....	26
Table 1-3 Titration results to determine negatively and positively charged groups.....	26
Table 3-1 Experiment design showing various ratios of Azido hydantoin and short chain QAC on the surface of fabric.....	38
Table 4-1 Active chlorine loading on PET-PMBAA -AzH surface after clicking QAS in various ratios.	45
Table 4-2 Contribution of cyclic N-H groups towards active chlorine loading in the mixed system	45
Table 4-3 Antibacterial results of 70/30 AzH/QAS and 70/0 AzH/QAS treated PET samples against CA-MRSA	49
Table 4-4 Antibacterial results of 70/30 AzH/QAS and 70/0 AzH/QAS treated samples against MDR- <i>E.Coli</i>	50
Table 4-5 Antibacterial efficacy of 70/30, 50/50 and 30/70 AzH/QAS samples against CA- MRSA	51
Table 4-6 Antibacterial efficacy of 70/30, 50/50 AND 30/70 AzH/QAS samples against MDR- <i>E.Coli</i>	52
Table 4-7 QAS immobilized on PET-MBAA/QAS surface with respect to dosage percentage	57
Table 4-8 Ratio of <i>N</i> -chloramine to QAS on PET-PMBAA-x%QAS surfaces.....	65
Table 4-9 Rate constant for the chlorination of modified PET fabric	67
Table 4-10 Antibacterial assessment of PET-PMBAA-QAS against CA-MRSA.....	68
Table 4-11 Antibacterial assessment of unchlorinated PET-MBAA/100QAS against CA-MRSA.....	69
Table 4-12 Active chlorine loading on PET-PA-AzH samples with and without positive charge	71
Table 4-13 QAC immobilized on PET-PA-AzH/QAS surface with respect to total clickable sites	73
Table 4-14 Ratio of <i>N</i> -chloramine to QAS on PET-PA-AzH/QAS surface.....	74
Table 4-15 Antibacterial test results of PET-PA 50/50 AzH/QAS and 50/0 AzH/QAS against <i>MDR E.coli</i>	75
Table 4-16 Antibacterial test results of PET-PA-70/30, 50/50 AzH/QAS and 30/70 AzH/QAS against <i>MDR E.coli</i>	75

LIST OF FIGURES

Figure 1-1 Classification of antibacterial surfaces	8
Figure 1-2 <i>N</i> -chloramine regeneration action	10
Figure 1-3 Regeneration principle	11
Figure 1-4 Concept of contact killing via “Polymer Spacer Effect”	18
Figure 1-5. Boosting microbiocidal function between cation and <i>N</i> -chloramine	28
Figure 3-1 Chemical synthesis of MBAA	33
Figure 3-2 Chemical synthesis of azido-hydantoin analogue.....	34
Figure 3-3 Chemical synthesis of QAC	35
Figure 3-4. Surface modification of PET fabric using MBAA monomer to form Semi-IPN followed by click reaction using antibacterial agents.....	37
Figure 3-5 Surface modification of PET fabric using PA monomer follow ed by click reaction using antibacterial agents	38
Figure 3-6 Structure of 4-(phenylazo) benzoic acid dye	41
Figure 3-7 Calibration curve of 4-(phenylazo) benzoic acid dye.....	42
Figure 4-1 Click reaction on PET-PMBAA surface with azido hydantoin analogue and QAS	44
Figure 4-2 Chlorination progress versus available chlorine in NaClO solution	47
Figure 4-3 Chlorination progress versus available chlorine in NaClO solution with addition of 1M NaCl at pH 8 for 1 hour	56
Figure 4-4 Zeta potential graph of PET-PMBAA-x%QAS samples	59
Figure 4-5 Zeta potential graph of PET-PMBAA-AzH/QAS and PET-PMBAA-QAS sample	61
Figure 4-6 Chlorination progress Vs time for PMBAA-PET-x% QAS surface	62
Figure 4-7 Surface charge density with respect to saturated active chlorine loading and conversion ratio ..	63
Figure 4-8 Surface charge density Vs percent active chlorine loading in 5 minutes	66
Figure 4-9 Chlorination kinetics graph showing Kobs for various ratios of QAS clicked on surface.....	67
Figure 4-10 Structure of Propargyl acrylate.....	70
Figure 4-11 Zeta potential graph comparing PET PA-AzH/QAS and PET-PA-AzH/QAS.....	72

1 INTRODUCTION

1.1 OVERVIEW

Cross contamination and outbreak of microbial infections has been a significant problem worldwide. The problem of rising antibiotic resistance has caught the world's attention. Infections caused by antibiotic-resistant bacteria have become more and more difficult to treat. While medicinal chemists are working at genetic level to combat resistance for improved treatment of infections caused by antibiotic-resistant bacteria^{1,2}, it is essential to ramp up our efforts in preventing those infections especially avoidable healthcare-associated infections (HAIs) from happening in the first place. HAIs are the infections that patients acquire while receiving treatment for another condition in health care facility and microbial infection is the most common cause of rise in incidence of HAIs^{3,4}. There are 1.7 million cases of HAIs each year in the United States resulting in approximately 99,000 deaths⁵. Major cause of nosocomial infection have been attributed to cross contamination through the hands of health care workers⁶. Gastmeier and his coworkers analyzed 1561 nosocomial outbreaks in the open database. They traced the source of 40.3% of the studied outbreaks back to index patients, 21.1% to contaminated equipment, and 19.8% to the environment. The major source of cross-contamination in hospitals is attributed to nursing uniforms , privacy curtains, and laboratory bench surfaces⁷. The contamination bedpans, floor, walls, washbasins, furniture and blood pressure cuffs was found to be as high as 58%⁸⁻¹⁰. Hospital floors were found to remain contaminated with *C. difficile* for up to 5 months¹⁰ and the

spread of methicillin resistant *Staphylococcus aureus* (MRSA) was found to happen via the unwashed hands of health care workers¹¹.

Studies have shown that microorganisms are capable of surviving for long durations in damp as well as dry conditions. The survival of clinically relevant bacteria on dry surfaces has been reported and researchers have found that most gram-positive and gram negative bacteria can survive for months on surface. Estimated duration of 1.5 hours – 16 months for *Escherichia coli* (*E.coli*)^{12,13}, 6 hours – 16 months for *Pseudomonas aeruginosa*(*P. aeruginosa*)^{14,15} and *MRSA*^{16,17} is shown to survive for 7days to 7 months. Lankford et al¹⁸suggested that textile surfaces in healthcare facilities can act as a reservoir for transferring bacteria to the hands of healthcare workers and found that bacterial strains could be recovered from upholstery even after cleaning.

Textile substrates may assist as a carrier for the transfer of bacteria to patients or hospital workers¹⁹ majorly contribute to HAIs. To break chains of bacterial transmission and prevent people from getting HAIs, it is vital to avert hospital high-touch surfaces as well as medical equipment from being reservoir of pathogenic microorganisms. Developing non-fouling or antibacterial surfaces might be a viable strategy to cut down bacterial cross-infection. Researchers have been developing novel approaches each year to prepare efficient antibacterial surfaces to minimize problems caused by bacterial infections. Three most widely adopted approaches include (Figure 1-1) a) surfaces that resist bacteria attachment rather than bacterial killing^{20–23} b) surfaces treated with leaching antibacterial agents where antibacterial compound leach out in the environment during use^{24–29} c) contact-active antibacterial surfaces which kills bacterial cells on contact without leaching the biocide. Based on literature review of approaches adopted to develop antibacterial surfaces, the contact-kill based antibacterial agents have been recognized as the most sustainable and environment friendly approach.

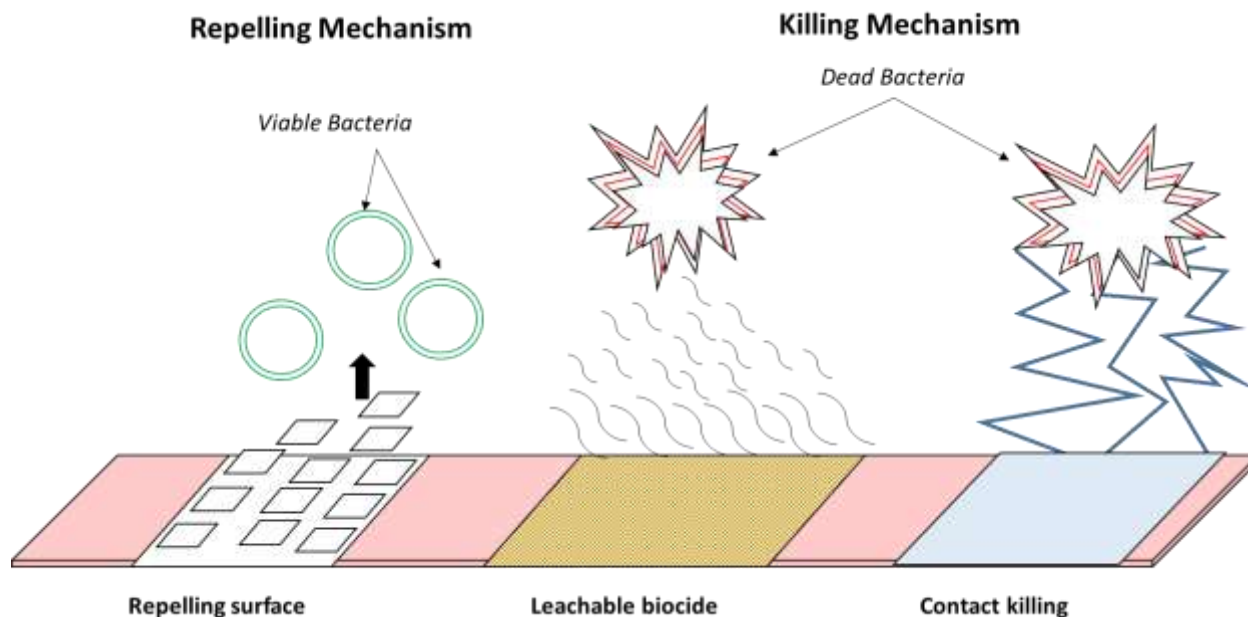


Figure 1-1 Classification of antibacterial surfaces

Tiller, Joerg C. Springer Berlin Heidelberg, 2010. 193-217³⁰

Contact- active surfaces can be created by fixing certain biocides onto them through covalent bonding and hence, are a sustainable alternative to the biocide leaching approach. Certain biocides can be attached irreversibly to a substrate to endow them with contact-kill property and hence, do not leach out upon use. The most widely studied contact-active antibacterial agents include *N*-chloramine and quaternary ammonium compounds (QACs). *N*-chloramines contain one or multiple N-Cl bonds in which Cl is partially positively charged and oxidative. Upon contact with bacterial cells, Cl^+ ions can transfer from *N*-chloramines to micro-organism cell wall to hinder metabolic functions in cells. The net results of the reaction between bacteria and *N*-chloramines are killed bacteria and conversion of *N*-chloramines to their precursor N-Hs. Chlorine bleaching of N-H, as the reverse reaction, can again convert precursor forms to biocidal *N*-chloramines. This serves as the basis for the rechargeable antibacterial property of *N*-chloramine grafted surfaces. Recently, it was found that covalently linked *N*-chlorohydantoin with QAC based cationic moiety could

result in a novel class of antibacterial agent with enhanced antibacterial efficacy on surfaces. Synergistic effect was not observed between surface bound long alkyl chain QAC and *N* – chloramine in previous studies but combination of short chain QAC with *N*-chloramine can produce a highly effective antibacterial activity³¹. In this project, an *N*-Chloramine and a short chain QAC(2-azido-*N,N,N*-trimethylethyl-1-ammonium chloride) will be grafted in particular ratios onto the surface of PET fabric to optimize the ratio of both components for most effective antibacterial efficacy, easiest recharging of treated surface and fastest recharging kinetics upon chlorination

1.2 CONTACT-ACTIVE ANTIBACTERIAL AGENTS

Contact-active antibacterial agents are the compounds which can be attached irreversibly to the substrate and hence, kill bacteria on contact without releasing the biocide. They are also known as non-leaching type biocides since the biocide does not leach out during use and hence, the environment does not get polluted. Also, contact active surfaces do not contribute to bacterial resistance as they either cause physical damage to the bacterial cells, or exert non-specific oxidative stress on bacteria rather than affecting specific targets such as ribosomes³². Contact-Active antimicrobial surfaces are usually engineered by physically or chemically attaching contact-active biocides to the substrate such as glass³³, polymer³⁴, metal³⁵ and paper³⁶ etc. The most commonly reported contact active antibacterial agents include *N*-chloramines, QACs such as alkyl pyridiniums, quaternary phosphoniums (QPs), carbon nanotubes and antibacterial proteins. This review will particularly discuss *N*-chloramines and QACs.

1.2.1 *N*-CHLORAMINES

N-chloramine based contact active antibacterial agents have gained significant research interests over the past two decade. Two different mechanisms have been suggested for biocidal

action of *N*-Chloramines. First mode of action states that the *N*-chloramine attack leads to the chlorination of the protein matrix in bacterial cells which does not necessarily result in bacterial killing. Second mechanism describes that *N*-chloramines penetrate into bacterial cells and it attacks various essential constituents through oxidation. These reactions denature proteins by transchlorination and eventually kill bacteria. The chances of inducing bacterial resistance through *N*-Chloramines are limited because they interaction with vital proteins in bacteria happens in a variety of nonspecific ways³⁷. Nagl et al³⁸ stated that resistance to *N*-chlorotaurine was not developed by strains of bacteria. Organic *N*-chloramines have been recognized as a class of effective biocides with broad inhibitory activities³⁹⁻⁴¹ and they can be divided into cyclic and acyclic based structures. Cyclic *N*- chloramines⁴² are efficient biocides and effective against broad-range of biocides. Acyclic *N*- chloramines⁴³ have also been synthesized and it was observed that acyclic structures could impart durable and rechargeable antibacterial property to treated surface.

1.2.1.1 RECHARGING ACTION

A reversible antimicrobial model was proposed by Gagliardi in 1961 which was only realized in 1998 when Sun identified *N*-Halamine chemistry onto fabrics. The reusable feature of *N*-halamine is the key factor for the suitability of such compounds as a potential antibacterial agent (Figure 1-2)

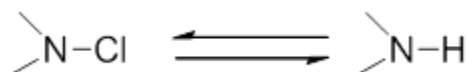


Figure 1-2 *N*- chloramine regeneration action

The conversion of N-H group to N-Cl is a reversible reaction and hence, the biocidal function on the surface can be repeatedly recharged using chlorinating agents such as chlorine bleach. In a study conducted by Sun et al.^{40,44} a new method of imparting cotton fabric with durable

and regenerable antimicrobial property was developed. This method utilized monomethylol-5, 5-dimethylhydantoin (MDMDH), a hydantoin derivative on cellulose and regeneration of biocidal property of MDMDH treated fabric through a laundering process using chlorine bleach. The regeneration principle has been depicted in Figure 1-3 as a reversible reaction which shows the regeneration ability by treatment with free chlorine as well as excellent stability of hydantoin ring.

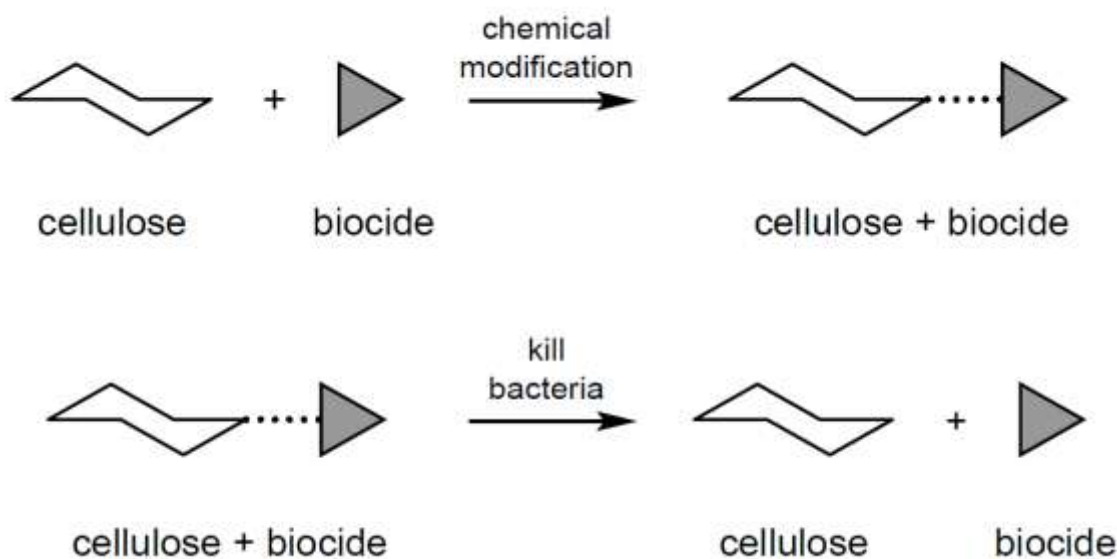


Figure 1-3 Regeneration principle

Sun, Gang, and S. Dave Worley. J. Chem. Educ 82.1 (2005) ⁴⁵

Rechargeability is the unique property of *N*-halamine (Figure 1-3) and it was observed that loss of chlorination–quench cycles lead to decreased amount regenerability and hence, subsequent decrease in antimicrobial efficacy. In a study conducted by Zhao and Liu et al , it has been reported that a better regenerability can be imparted by forming the thermoplastic semi-Interpenetrating network (IPN) using a nonhydrolyzable cross-linker⁴⁶. IPN is considered as a successful method to modify the surface of highly inert semi crystalline thermoplastic polymeric substrates by using a functional monomer and a crosslinker to form a 3-D interlocking structure. This study demonstrated the effect of cross-linker towards the durability of IPN which is based on the regenerability of *N*-

halamine by using three types of cross-linkers i.e. divinylbenzene (DVB), methylenebisacrylamide (MBA) and 2-ethylene-glycol diacrylate (EGDA). It was found that treated fabric involving use of DVB as cross-linker showed significantly better antibacterial regenerability.

In another study, Bisquera and Sumera⁴⁷ reported monoformylated 5,5dimethylhydantoin or monomethylolhydantoin were synthesized and grafted to polyurethane prepolymer composed of castor oil and toluene diisocyanate. The synthesized polyurethane coatings could be readily converted to regenerable biocidal *N*-halamine structures by treatment with chlorine bleach and exhibited antimicrobial effects against *E.coli*, *S.aureus*, and *C.albicans*. Coatings with 10% by weight hydantoin derivative and two hours soaking time in acidified 20% by volume chlorine bleach showed sufficient oxidative chlorine loading that remains biocidal for at least 5 days.

1.2.1.2 CONVERSION RATIO OF CYCLIC AND ACYCLIC N-H TO N-CL

Antibacterial properties of cyclic *N*-chloramine have been utilized to develop durable and rechargeable antibacterial textiles. Cyclic *N*- chloramine possess various advantages such as rapid killing of bacterial strains, great stability in a broad range of pH and temperature, and rechargeable property using chlorine bleach^{48,49}. The *N*- chloramine family was expanded by synthesizing acyclic *N*-halamine structures which were reported to have comparable antimicrobial property as that of cyclic *N*-halamines. Acyclic *N*-halamines represents another class of *N*-halamine structure which can be employed onto polymeric or textile substrates^{43,50}. Various studies describe treatment of cotton by grafting of cyclic & acyclic *N*-halamine structures and the low conversion of N-H to N-Cl has been recognized as a major challenge.

The conversion ratio was quite less than available amides on the surface. The possible reasons have been identified through the course of time. Liu et al⁴³ grafted two vinyl amide monomers acrylamide (AM) and Methacrylamide(MAM) onto cellulose via free radical

polymerization process. The possible reason of low conversion was that the initiators added during grafting process could either initiate hydrogen abstraction from cellulose to form tertiary carbon radicals or initiate radical addition on vinyl monomer producing homopolymer. High grafting efficiencies on the cellulose indicated the predomination of hydrogen abstraction process. Another observation revealed that acyclic chloramines were sensitive to alkaline conditions.

In another study Liu et al⁵¹ in 2008 identified the reason of low conversion of acyclic N-H to N-Cl upon chlorination especially in case of radical polymerization of acrylamide on cotton in the presence of potassium persulfate (PPS) . It was found that imidization reaction was the prominent side reaction responsible for the low N-H conversion to N-Cl. Elimination of HCl from acyclic N-Cl leads to formation of imide ($\text{N}=\text{C}$) structures and vicinal CH does not allow conversion of N-H to N-Cl. Also, hydrolysis of secondary amide was responsible for loss of amide groups grafted on cotton. As a solution it was proposed that amount of the initiator in the grafting process should be reduced and employing initiators that do not lead to hydrogen abstraction from amide group can also reduce the side reaction. In 2009, Liu et al⁵¹ proposed a method to overcome hydrolysis of primary amides upon chlorination especially under alkaline conditions. It was concluded that hydrolysis was significantly reduced by addition of electrolytes such as NaCl under slightly basic conditions. In addition to this, use of non-hydrolysable components was suggested by Zhao et al⁴⁶ such as Divinylbenzene(DVB) which was recognized as non- Hydrolysable crosslinker. So far, 3-11% conversion of N-H incorporated using acyclic *N*-halamine precursors to N-Cl could be observed whereas 20-30% conversion of N-H to N-Cl was observed by grafting cyclic *N*-halamine structures. This conversion ratio is significantly less than expected number and there is a scope of improvement.

1.2.1.3 MODIFICATION TECHNIQUES

Sun et al⁵² developed durable and regenerable antibacterial cotton as well as polyester/cotton blended fabrics by using 2-10% dimethylol dimethylhydantoin (DMDMH) in a pad-dry-cure based chemical finishing process. The add-on rates of hydantoin groups on fabrics were significantly high and resulted in a durable antimicrobial functionality upon chlorination using diluted chlorine bleach. Biocidal properties were regenerable by treatment with chlorine bleach in laundry and were durable for over 50 standard machine washes. In a similar study, Chen et al⁵³ synthesized 2-amino-4-chloro-6-hydroxy-s-triazine (ACHT) through controlled hydrolysis of 2-amino-4,6-dichloro-s-triazine (ADCT) and ACHT was immobilized on cotton cellulose using simple pad-dry-cure approach. After chlorination, rechargeable biocidal activities against gram-positive and gram-negative bacteria were observed. Coating technique was adopted by Kou et al⁵⁴ where monomers 6-phenyl-3-(3-triethoxysilylpropyl)-1,3,5 triazinane-2,4-dione and 6,6-dimethyl-3-(3-triethoxysilylpropyl)-1,3,5-triazinane-2,4-dione were synthesized to coat cotton fabric.

Ren et al⁵⁵ synthesized *N*-halamine precursor 3-(4-vinylbenzyl)-5,5-dimethyl hydantoin (VBDMH) and grafted on cotton fabrics using cetylmethylammonium bromide (CTAB) via admicellar polymerization. Admicellar polymerization includes three-step process. The first step is admicellar formation, second step is adsolubilization and third step involves a polymerization reaction with the aid of water soluble initiators. As soon as the polymerization reaction is done, the surfactant is removed by washing with copious amount of water. The treated fabric was very effective to inactivate both *S. aureus* and *E.coli*.

Recently, a new method of surface modification on highly inert PET surface was reported which involves deposition of the polymers on PET surface by the formation of an interpenetrating network^{46,56}. Liu et al⁵⁷ modified the surface of PET by forming thermoplastic semi-IPN. The term

semi-IPN is justified because the polymer chains in semi-crystalline polymers were able to pass through numerous amorphous and crystalline portions. In this case, the crystalline portions act as physical cross-linking points in the polymer. PET fabrics were modified using vinyl amide monomers, crosslinker N,N'-methylenebisacrylamide (MBA) and photo-initiator Benzophenone (BP) which was swollen in methanol. The results demonstrated that PAM-PET fabric could achieve a total reduction of 10^5 – 10^6 CFU mL⁻¹ of MRSA in 10 min.

1.2.2 QUATERNARY AMMONIUM COMPOUNDS

QACs are cationic agents known for their odor removal, hard-surface cleaning and antimicrobial properties. These compounds can reduce surface tension of water and possess properties such as attracting negatively charged moieties like bacteria. QACs were first synthesized by Menschutkin in 1890 and the 'Menschutkin reaction' is still considered as the most suitable method for the synthesis of QACs. Depending on length of substituting alkyl chain, QACs can be divided into long chain and short chain QACs. According to Inacio et al, QAC is considered long chain when its alkyl substitution reaches longer than 12 carbon chains whereas alkyl chain shorter than 12-carbons is considered as short chain QAC⁵⁸. Gozzelino et al. describes alkyl chain length of 8 or longer as long chain QACs⁵⁹ and Li et al has also considers alkyl chain longer than 6 as long chain QACs³¹.

1.2.2.1 EFFECT OF ALKYLATION ON ANTIBACTERIAL ACTIVITY

QAC's have been recognized in literature to show antibacterial activity depending on length of carbon chain. Various researchers have reported optimum alkyl chain length of QAC's suitable for considerable activity when the compound is used on polymer substrate. Literature study with respect to effect of alkylation on antibacterial activity reveals that with the growth in alkyl chain,

several features polymer behavior change. There is an increase in the adsorption/absorption ability and lipophilicity but this leads to variation of hydrophilic-hydrophobic balance that can result in variation of killing ability against range of microorganisms

Gozzelino et al. in 2011⁵⁹ published an article where antibacterial activity of QAC's was determined in both solution and non-leachable coatings as a function of the alkyl chain length. Quaternary ammonium monomers (QAMs) possessing a polymerizable acryloyl functional group and alkyl chains with 2, 8 and 16 carbons (termed as QAM-C2, QAM-C8 and QAM-C16 respectively) were synthesized and coated onto stainless steel coupons. The coating formulations included a photoinitiator, a urethane-diacrylate oligomer, a crosslinker and QAMs. The antibacterial activity of modified steel coupons was tested against *E. Coli*, *S. aureus*, and *Listeria monocytogenes* strains by following the Japanese Industrial Standard Test (JIS Z 2801). It was found that steel coupon bound with QAM-C8 was the most effective biocidal surface against the above mentioned three strains with 2 hours of contact. The activity of QAMs in solution demonstrated that both C8 and C16 were found to be effective against the three tested pathogens and different types of QAMs follow the bactericidal order QAM-C8 \approx QAM-C16 > QAM-C2.

In another study published by Gozzelino et al. in 2011⁶⁰, a similar acrylate formulation was used to incorporate QAMs into solid film coatings through UV-initiated photo polymerization. The biocidal property of the polymer films containing QAMs was assessed against *E.coli* and *S.aureus*: according to ISO 22196 method designed for the evaluation of antibacterial activity on plastics and other non-porous surfaces). This time, the authors conducted thorough water extraction of unbound QAMs from the coatings and found that the biocidal efficacy of the coatings dramatically decreased after water extraction. Bacterial reduction of *E. coli* and *S. aureus* was less than 1 log after 24 hours contact on all the coatings (QAM7, 8, 10 and 12) except on the coating containing QAM16. The

acrylate coatings containing 5%, 10% and 20% of QAM16 resulted 2.8, 4.8 and 8.5 log reduction of *S. aureus* within 24 hours of contact. The authors speculated that the higher hydrophobicity of QAM16 contributed positively to the contact kill of bacteria.

1.2.2.2 CONTACT ACTIVE QACS - MECHANISM OF ACTION

The antibacterial mechanisms of QACs have been explored over the time and explained by various researchers. Although Isquith et al⁶¹ introduced the concept of contact-active antibacterial surfaces in 1972, the mechanism of action of surface bound QACs was not clear until recently. In 2001, Tiller et al³³ introduced a mechanism stating that antibacterial effect was caused due to hydrophobic interactions of hydrophobically modified substrate with bacterial cell membrane. The most recent working mechanism till 2001 was polymeric spacer effect (Figure 1-4) that allows the antimicrobial groups immobilized on the long spacer to penetrate the cell wall of an attached microorganism and reach the inner cell membrane to eventually kill the cell⁶².

The concept of polymeric spacers has been questioned because the mechanism was difficult to imagine and active alkyl chain lengths i.e. C6 and C8 of the grafted polymers would require high stretching of spacer to reach the inner cell membrane of target microorganisms. This explanation was evident from the study conducted by Huang et al⁶³ who described that the surfaces bonded with short QA chains having DP 97 which accounts to nearly 24 nm was found to possess biocidal activity. Since the thickness of cell envelope (46 nm) was more than length of this QA. This study proved that killing mechanism of QA groups was not based on penetrating the cell membrane. Similarly, in number of studies the polymeric spacer effect has not been considered as the working mechanism for contact killing based on quaternary ammonium groups⁶⁴⁻⁶⁶.

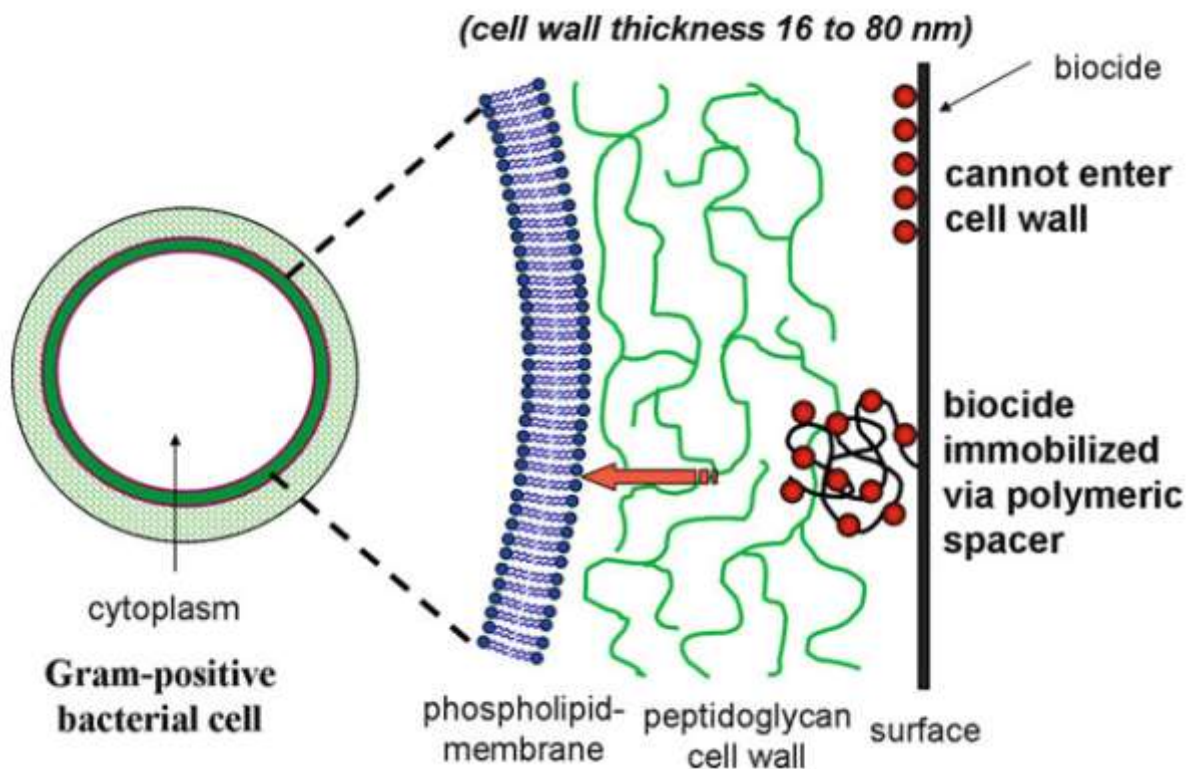


Figure 1-4 Concept of contact killing via “Polymer Spacer Effect”

Tiller, Joerg C. Springer Berlin Heidelberg, 2010. 193-217³⁰

Another mechanism was proposed by Kugler et al in 2005⁶⁷ who proposed Ion-Exchange mechanism for bacterial killing and this model states that exchange of divalent cations present on outer membrane of bacteria with cations present on charged surface. This exchange of ions leads to destabilization and loss of natural counterions of bacteria leading to cell death. For example, in the case of *E.coli*, stabilization of outer membrane is partially provided by divalent cations i.e. Mg^{2+} and Ca^{2+} which are removed during adsorption of bacteria on charged surface. Study reported by Huang et al⁶³ support this mechanism by showing antibacterial efficacy of surface bound QA groups against both gram negative and gram positive bacteria. Also Murata et al⁶⁸ shows killing of *E.coli* based on ion-exchange rather high density surfaces killing bacteria through cell penetration.

Another study favouring phospholipid sponge effect was reported by Asri et al in 2014⁶⁹. This group confirmed that killing mechanism of QACs immobilized on surface is different from QACs in dissolved solution. In the case of immobilized QACs, shape-adaptive coatings were prepared to enhance the contact area with adhering bacteria and existence of positive charge generated an electric field leading to locally enhanced strong forces of attraction between surface and anionic-lipids in bacterial envelope. These lethal forces led to the removal of membrane lipids and caused cell death. On contrary, the action of QACs in solution was suggested to be based on the interdigitation of membrane across the entire bacterium surface. Additionally, Asri et al. confirmed that presence of lethally strong adhesion force correlates with the finding that QACs immobilized on surface possess antibacterial active when the positive-charge density is above a critical threshold. This study does not support the counter ion-exchange mechanism of bacterial-killing as proposed by Kugler et al. and shows that immobilized QACs can kill bacteria attached to surface despite the presence of surrounding Ca^{2+} ions which may hinder replacement of Ca^{2+} ions. Although sponge effect has been supported by several authors, this model could not provide sufficient explanation concerning the release of water insoluble phospholipids from cell wall towards the antibacterial surface.

1.2.2.3 CHARGE DENSITY THRESHOLD ON SURFACE FOR OPTIMUM ANTIBACTERIAL EFFICACY

The literature study reveals that charged surfaces, particularly cationic surfaces, can kill bacteria upon contact and bacterial death occurs quickly after adhering to substrate bearing cationic group above a particular charge-density threshold. Quaternary ammonium compounds are most extensively used for imparting positive charge to surface. There are few reports on the optimum charge-density threshold of cationic surfaces required to impart desired antibacterial activity.

In a study conducted by Murata et al. in 2007⁶⁸, suggested that surface charge density plays a major role in preparing surfaces for maximum killing of bacteria. Results demonstrated that a surface is able to kill a monolayer of *E. coli* cells when cationic charge density on surface becomes greater than 5×10^{15} charges/cm². Interestingly, the author established a correlation between measurements of the *E. coli* surface charge and charge density on cationic surface which shows that magnitude of *E. coli* surface charge is between 5×10^{14} and 5×10^{15} charges/cm². In 2008, Huang et al.⁶³ elucidated the effect of surface positive charge density on antibacterial activity. Experimental data revealed that when the density of surface QA groups increased from 1.0×10^{14} unit/cm² to 6.0×10^{14} unit/cm², number of *E. coli* killed by the surface increased from 0.06×10^5 units/cm² (nearly 10% kill) to 0.6×10^5 units/cm² (97% kill). Overall, it was concluded that biocidal activity of surfaces varies with the amount of QA grafted on surface whereas the killing capacity of all QA surfaces was found to be similar showing 1×10^{10} units of QA required to kill one bacterium. The charge density threshold described in this study was similar in magnitude to the threshold study conducted by Kugler et al.⁷⁰. Kuglar et al conducted an experiment where glass surfaces were grafted with quaternized poly (vinylpyridine) chains and varied the charge density between 10^{12} and 10^{16} positive charges/cm² within organic layer. ‘Outer layer charge density’ (OLCD) was estimated considering that the charges were distributed homogeneously throughout the polymer layer. Moreover, OLCD was compared to the negative charge density on the bacterial envelope. It was found that it is necessary to have an OLCD of 10^{14} N⁺ cm⁻² for *S. epidermidis* and *E. coli* in low division conditions. In high-division conditions, lower charge density was required which was of the order of 10^{12} N⁺ cm⁻² for *E. coli* and 10^{13} N⁺ cm⁻² for *S. epidermidis*.

1.2.2.4 MODIFICATION TECHNIQUES

Quaternary ammonium compounds have been attached to the surface of potential substrates using various techniques, out of which chemical method via grafting technique and click chemistry, physical method via coating and plasma polymerization have been used most widely.

Lee et al in 2004³⁶ proposed a method for developing highly effective non-leaching antimicrobial surface using quaternized polymer chains produced by ATRP “Grafting from” technique. The main idea behind using ATRP was to graft well defined polymers with predictable molecular weights and narrow distribution of MWs from surfaces to yield high degree of functionality. High concentration of QA groups on polymer surface resulted when PolyQA was covalently attached to the surface of paper or glass slides through immobilization of an ATRP initiator and polymerization of 2-(dimethylamino)ethyl methacrylate (DMAEMA). Finally quaternization with ethyl bromide was performed. The success of proposed method was revealed by substantial antimicrobial activity of treated surfaces against *E.coli* and *Bacillus subtilis* as well as the persistent antibacterial activity even after repeated use of modified glass.

In contrast to above mentioned approaches, Huang et al in 2008⁶³ used “Grafting onto” technique to develop antimicrobial surfaces. In this study, antimicrobial glass surfaces was prepared by the “grafting onto” technique using polyacrylate based block copolymers prepared by ATRP. Glass surface was immobilized with copolymers by reacting trimethoxysilyl groups in the copolymers with silanol groups on the glass surface. Lastly, the pendant amino groups were converted to QA with ethyl bromide.

Gozzelino et al⁶⁰ used a coating method to introduce antibacterial properties into solid films by means of UV initiated photo-polymerization. A liquid coating was converted to solid polymer network by initiating crosslinking co-polymerization of a mixture of liquid monomers, a crosslinker

and a photo-initiator using UV radiation. The coating formulations consisted of a UV cross-linkable oligomer that can be layered on a substrate without the use of solvents and QAMs capable of imparting biocidal properties to coatings.

Xu et al in 2013⁷¹ prepared antibacterial surface on cellulosic material using a “clickable” quaternary ammonium compound i.e. N-(2-ethoxy-2-oxoethyl)-N,N-dimethylprop-2yn-1-aminiumbromide (EdMPABr). EdMPABr can be covalently attached to surfaces containing azido group through click reaction (specifically Cu(I)-catalyzed alkyne-azide cyclo-addition reaction), generating surfaces possessing non-leaching antibacterial agents. Li et al⁷² also used click chemistry to covalently attach a composite biocide with both QAC and *N*-chloramine moieties onto PET and cotton surface. PET bearing clickable alkyl handle was subjected to surface modification through Semi-Interpenetrating Network approach³¹

1.3 CHARACTERIZATION STUDY

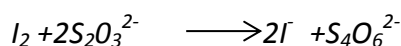
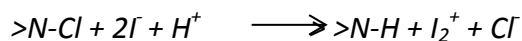
1.3.1 CHARACTERIZATION OF *N*-HALAMINE

Physical and chemical methods for characterization *N*-halamine bonds i.e. ($>N-X$) have been described in literature. Physical methods include techniques such as Fourier transform infrared spectroscopy (FTIR), X-ray photoelectron spectroscopy (XPS), nuclear magnetic resonance spectroscopy (NMR) and chemical reactions involve characterization using Iodometric-Thiosulfate Titration and reaction with Methionine

Chen and Sun et al⁷³ characterized the conversion reaction of 5,5-dimethylhydantoin (DMH) to 3-dodecyl-5,5-dimethylhydantoin(DDMH) and then to Cl-DDMH using proton NMR and FTIR analyses. In the H-NMR spectra, there was an amide proton signal at 5.8 ppm for DMH and DDMH. This proton signal was not present in Cl-DDMH which indicated that the N-H bond in

DDMH was transformed into N-Cl group. The FTIR spectra of DMH and DDMH had shown a broad peak at 3280 cm^{-1} representing N-H stretching vibrations. This peak was not observed in the spectrum of Cl-DDMH which shows successful N-H into N-Cl conversion. For Cl-DDMH, there were two new bands at 758 and 735 cm^{-1} showing N-Cl bond and shifting of C=O band from 1782 and 1707 cm^{-1} in DDMH to 1794 and 1728 cm^{-1} in Cl-DDMH was observed due to breakage of hydrogen bond in the amide group in the DDMH molecule.

A well-established chemical method has been used to determine the active chlorine loading on surface by iodometric titration where iodide ions are oxidized by chlorine leading to the release of iodine, which is then titrated against thiosulfate as per following equation



Cao et al⁷⁴ calculated the active chlorine content of the chlorinated surface by the method based on following equation:

$$[Cl+]\% = \frac{35.45}{2} \times \frac{(V_{Cl} - V_0) \times 10^{-3} \times N}{W_{Cl}} \times 100$$

V_0 - control reading, V_{Cl} – Burette reading (volume of KI consumed), W_{Cl} - weight of fabric used for titration, N – normality of solution.

1.3.2 CHARACTERIZATION OF QACs

1.3.2.1 METHOD TO DETERMINE SURFACE ACCESSIBLE QUATERNARY AMINES

A well-defined approach described in this section has been followed by researchers to evaluate surface accessible quaternary amine. It was found that the anionic dye fluorescein binds

selectively to QA groups but not to tertiary or primary groups⁷⁰. The modified surfaces containing QA groups (1x1 cm²) were kept in a 10mL of a 1wt% solution of fluorescein in distilled water for 10 min. The fluorescein solution was collected and the samples were thoroughly rinsed with distilled water. Samples were then placed in a fresh tube containing 3mL of 0.1% solution of cetyltrimethylammonium chloride. In order to desorb the dye, the samples were kept on an orbital shaker for 20 min at 300 rpm. 10% v/v of 100mM phosphate was added to the resultant solution and its absorbance was measured at 501nm. The amount of fluorescein bound to the surface was calculated using the extinction coefficient of 77mM⁻¹cm⁻¹.

1.3.2.2 ZETA POTENTIAL MEASUREMENT

The zeta potential of polymer substrates can be used to describe the surface behaviour in the presence of an aqueous solution. These values represent the nature as well as dissociation of reactive functional groups explaining their hydrophilicity, polarity or hydrophobicity of the material^{75,76}. High surface charge density originates from the functional groups present on a modified polymer surface unlike untreated polymer surfaces. This type of charged solid surface when comes in contact with a liquid phase leads to generation of an electrical potential at the interface. As a result, a double layer is formed: Surface bound liquid phase ions of opposite charge and surface bound ionizable groups forms fixed layer whereas loosely bound liquid phase ions forms the mobile layer. The change in potential across this double layer is known as zeta potential⁷⁷. Zeta potential depends on pH, valence and size, counterions concentration, temperature, material and its surface properties, etc^{78,79}. Zeta potential can also be used to determine isoelectric point (IEP), the point at which the electro kinetic potential becomes zero. Zeta potential is a tool used to differentiate different kinds of polymer substrates due to their different polarity since ζ -potential originates due to preferential adsorption OH⁻ or H₃O⁺ ions on the surface.

1.3.2.3 REFERENCE DATA CONCERNING POSITIVELY CHARGED SURFACES

Adhesion of bacteria to the substrate has been evaluated by Gottenbos et al⁸⁰ where they studied the antimicrobial efficacy of positively charged surfaces on gram-positive and gram-negative bacteria. The antimicrobial effects were studied by comparing positively charged poly(methacrylate) and (PMMA/TMAEMA-Cl) surface (12 mV) with those of negatively charged poly(methyl methacrylate, PMMA) (−12 mV) and PMMA/MAA(−18mV) surface was studied as shown in Table 1-1. It was observed that positively charged surfaces helps in faster adhesion of bacteria.

Farber et al⁸¹ studied Antimicrobial activity of QA Polyethyleneimine (QA-PEI) where they explained the methods to quantify elemental composition of organic sample, particle size as well as surface characteristics such as zeta potential. QA-PEI nanoparticles were synthesized by reductive amination followed by *N*-methylation to raise the positive charge by converting PEI's primary, secondary and tertiary amino groups into quaternary ammonium groups.

Table 1-1 Initial deposition rate, percentages of growing bacteria of gram-positive and gram-negative bacteria on polymer films with varying charge density

Strain	Charge	Initial deposition rate (cm ² /s)
S. aureus	- -	1600
	-	1780
	+	2700
E. coli	- -	240
	-	720
	+	1720

Table 1-2 Characterization of QA-PEI nanoparticles at different degrees of alkylation

Sample	Degree of alkylation	Inhibition concentration $\mu\text{g/mL}$	Elemental analysis			C/N	Zeta potential mV
			%N	%C	%I		
1	1:1	40	7.03	32.74	54	3.61	85
2	1:0.75	40	9.05	33.63	49.25	3.16	60
3	1:0.5	80	8.85	30.94	54.25	2.81	72
4	1:0.25	160	9.26	29.60	53.70	2.45	80

The Table 1-2 shows data obtained with QA-PEI substituted with various degrees of octanal. A study conducted by Schaep et al ⁸² explained the charge evaluation of nanofiltration membranes. The surface charge of four commercially available nanofiltration membranes was calculated and compared. Titration method was used to distinguish between positively and negatively charged groups on the membrane surface by determining ion-exchange capacity. Also, charge density at the outer membrane surface was evaluated by calculating zeta potential.

Table 1-3 Titration results to determine negatively and positively charged groups

Membrane	Negatively charged groups (eqm^2)	Positively charged groups (eq m^2)
NTR7450(sulfonated polyethersulfone)	2.0×10^{-4}	1.9×10^{-5}
CA 30 (Cellulose acetate)	8.9×10^{-5}	1.8×10^{-5}
NF 40 (Polypiperazine-amide)	3.1×10^{-5}	$<0.8 \times 10^{-5}$
UTC 20 (Polypiperazine-amide)	2.5×10^{-6}	1.3×10^{-5}

The NTR 740 surface carried the highest number of negatively charged groups. This is because topmost layer of this membrane contained sulfonic acid groups. Sulfonic acid groups (–

SO³⁻) present on the NTR 7450 membrane were strongly acidic and were completely dissociated over the full pH range. The carboxylic groups (–COO–) present on polyamide as well as on cellulose acetate membranes were weakly acidic and could not be dissociated at a low pH.

1.4 COMBINED ACTION OF *N*-CHLORAMINE AND QUATERNARY AMMONIUM COMPOUND

Combined effect of QAC and *N*-chloramine was studied by Li and Liu et al³¹ and found that a positive charge contributes to a faster killing of bacteria as compared to a negative charge. They synthesized non-ionic and ionic derivatives of a *N*-chloramine precursor 5,5-dimethyl hydantoin (DMH) with clickable azido handle and bonded them onto cotton and PET surfaces. After converting the surface bound DMH to *N*-chloramine with dilute NaClO, the authors challenged the specimens with clinical relevant strains of *E. coli* and *MRSA* by following the “sandwich” version of AATCC 100 method. It was found that a short-chain (methyl) QAC charge center facilitate the kill of both bacteria despite that the short-chain QAC itself is not biocidal. There was, interestingly, no synergistic effect between surface bound antibacterial long chain QAC (C12) and *N*-chloramine. The “boosting effect” of short-chain QAC towards the antibacterial efficacy of *N*-chloramine was speculated to arise from electrostatic attraction as shown in Figure 1-5. The negatively charged bacteria could be arrested by the cations through electrostatic interaction which facilitates the oxidative chlorine transfer to the cell’s biological receptors leading to bacterial death. In this study, 1:1 ratio of *N*-chloramine and QAC on PET/cotton surface were used and the antibacterial effect was studied based on this combination. This 1:1 ratio might not be considered optimum for most effective antibacterial efficacy as well as highest conversion of surface bound N-H to N-Cl. In order to find the optimum ratio of *N*-chloramine and QAC on fabric surface, various combinations of

these two components should be investigated to provide further insight into contribution of positive charge and most desirable antibacterial property.

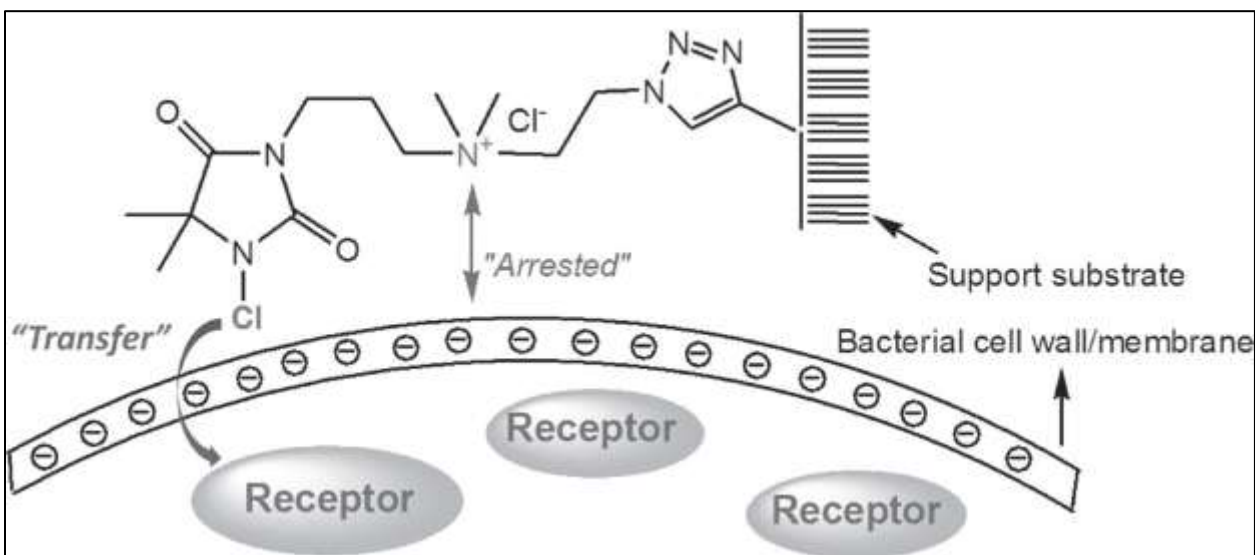


Figure 1-5. Boosting microbiocidal function between cation and *N*-chloramine

Li, Lingdong, et al. Advanced healthcare materials 1.5 (2012): 609-620³¹

1.5 GAP IN CURRENT LITERATURE

During the past few decades, a lot has been done concerning the development of novel antibacterial agents to minimize microbial infections. Contact-active antibacterial agents such as *N*-halamine and Quaternary ammonium compounds have been recognized as effective antibacterial agents. Despite multiple efforts to discover ideal antibacterial agents, limited study has been done related to combined use of various antimicrobial agents having different modes of action ("Combined Chemistry") on material surfaces to improve the efficiency of these antimicrobial agents and fight against resistant strains of bacteria. Current literature available in terms of combined use of *N*-halamine precursor and short chain QAC states is very limited and only 1:1 ratio on the surface of fabric has been tested. This has been identified as a gap in the study and the

optimum ratio of *N*-halamine/QAC on the surface of fabric can be identified to broaden the horizon of combined chemistry application. The contribution of positive charge towards antibacterial efficacy can be studied in a detailed manner. With respect to surface bound *N*-chloramines, the conversion of N-H to N-Cl has been reported from 3-11% which is quite low. Positive charge might contribute to increased conversion of surface bound N-H to N-Cl.

1.6 CONCLUSION

Designing antibacterial surfaces has become extremely important to minimize the Healthcare Associated Infections which is a major cause of mortality worldwide. Contact-active antibacterial surfaces have gained much importance based on their non-releasing property owing to the covalent attachment of biocides onto surfaces. Out of various contact-active based antibacterial agents, *N*-chloramines and QACs have been most widely studied due to their promising antibacterial activity and wide applicability. The combined use of different antibacterial chemistries would help generate novel antibacterial agents to fight against resistant strains. Recently, antibacterial surfaces have been engineered by combined use of *N*-chloramine and QAC by Li et al³¹ and this work is the first attempt of studying the combined antibacterial effect of *N*-chloramine and QACs on surfaces. It was found that 1:1 ratio of *N*-chloramine and short chain QAC on PET/cotton surface resulted in faster killing of bacteria due to electrostatic interaction between negatively charged cell wall and cationic charge centre of QACs. This study confirmed that introduction of positive charge could result in higher conversion of surface bound N-H to N-Cl as well faster killing of bacteria. There is a further scope of investigating various other combinations of *N*-chloramines and QAC on fabric surface to optimize the ratio of two components assisting in-depth study of contribution of positive charge for most effective antibacterial property.

2 HYPOTHESIS AND OBJECTIVES

The development of antibacterial surfaces to minimize cross contamination and HAIs has become one of the highest research priorities. Non-leaching antibacterial agents have emerged as the most efficient and environment friendly approach to render surfaces antibacterial. There is not enough research conducted on combined use of different kinds of antibacterial agents on surfaces. The first attempt to study combined use *N*-chloramine and positively charged QAC on fabric surface was initiated by “Biomaterials synthesis and surface engineering lab” and so far 1:1 ratio of these two components on surface has been investigated. It has been confirmed from the previous study that immobilization of short chain QAC bearing positive charge on cotton surface facilitated faster killing of bacteria and higher conversion of surface bound N-H to N-Cl as compared to the surface without positive charge. It is hypothesized that there is an optimum ratio of *N*-chloramine and QAC which might not be 1:1 for the highest conversion of surface bound N-H to N-Cl and the most effective antibacterial efficacy.

In this study, various ratios of *N*-chloramine and short chain QAC were immobilized on PET surface and in-depth study relating contribution of positive charge was conducted. The project aims to achieve the following goals and fill the gap in the current literature.

1. Develop a method to covalently bond a short-chained QAC (2-azido-N, N, N-trimethylethyl-1-ammonium chloride) and an *N*-chloramine (3-(3-azidopropyl)-5,5-dimethylimidazolidine-2,4-dione) in a variety of ratios onto PET fabrics.

2. Determine the contribution of positive charge through the short –chained QAC on the surface of fabric towards enhanced conversion ratio of N-H to N-Cl as well as faster killing of bacteria as compared to PET surface without positive charge.
3. Identify the ratio of *N*-chloramine and QAC on the surface of PET fabric (out of various ratios tested in this study) for the most effective antimicrobial activity and the highest conversion of surface bound N-H to N-Cl.
4. Perform the chlorination kinetics of PET fabric immobilized with various ratios of QAC and *N*-chloramine

Specifically, I have performed surface modification PET and immobilize *N*-halamine and QAC on PET surface in known ratios through “click chemistry”. The treated PET was tested for its antibacterial activity and active chlorine loading on surface. The amount of positive charge on the surface was also quantified using dye titration method and zeta potential values. The ratio of *N*-halamine and QAC (out of various ratios of N-Cl and QAS tested) showing highest antibacterial activity is identified.

3 EXPERIMENTAL DESIGN

The surface of chemically inert PET will be modified by the formation of Surface Interpenetrating Network particularly thermoplastic semi-IPN in the current study. *N*-chloramine (5,5-Dimethylhydantoin) and quaternary ammonium compound (QAC) will be attached to the semi-IPN PET fabric surface by click reaction. Click chemistry is considered to be an attractive method to impart functionality to surface due to its high reactivity, mild reaction conditions and good selectivity. The ratio between *N*-chloramine and quaternary ammonium compound (QAC) will be varied to find the most efficient antibacterial properties.

3.1 MATERIALS

Woven plain PET, no. 777H was purchased from Test Fabrics, Inc., West Pittston, PA/United States. All solvents and chemicals such as 5,5-dimethylhydantoin, N, N'-methylenebisacrylamide, benzophenone, propargyl acrylate, 1,1-dimethylpropargylamine, acryloyl chloride, 1,3-dibromopropane were purchased from either Sigma-Aldrich or Fisher. Monomer MBAA, azido hydantoin analogue and QAC were synthesized following published protocols^{72,83}. Also, MBAA was purchased from GVK, Hyderabad, India.

Community-associated (CA)-*MRSA* #40065 and multi-drug resistant (MDR) *E.coli*# 70094 were used to challenge all the biocide substrates and these strains were obtained from the Canadian Ward Surveillance (CANWARD) study evaluating antimicrobial resistance in Canadian hospitals. Tryptone Soya agar was purchased from Sigma-Aldrich.

3.2 SYNTHESIS OF MONOMER AND BIOCIDES

3.2.1 SYNTHESIS OF N-(2-METHYLBUT-3-YN-2-YL) ACRYLAMIDE (MBAA)

180.6 mmol of 1,1-dimethylpropargylamine and 198.62 mmol of triethylamine were dissolved in 100 mL dichloromethane. 200 mmol of acryloyl chloride was dissolved in 50 mL of dichloromethane and was added to the mixture dropwise in 0.5 h at 0°C. The reaction continued at room temperature for 24 hrs. Triethylamine salt was removed by crystallization in ethyl acetate followed by column purification⁸³. The synthesis reaction is shown in **Error! Not a valid bookmark self-reference.** ¹H NMR (CDCl₃) δ 1.69 (s, 6 H, 2 CH₃), 2.35 (s, 1 H, ≡CH), 5.62 (dd, J = 10.2, 1.4, 1 H, =CHH), 5.70 (bs, 1 H, NH), 6.04 (dd, J = 16.9, 10.2, 1 H, =CH(CO)), 6.29 (dd, J = 16.9, 1.4, 1 H, =CHH); MS m/z 137 (M⁺, 8), 136 (47), 122 (22), 68 (100). Anal. Calcd for C₈H₁₁NO: C, 70.04; H, 8.08; N, 10.21. Found: C, 70.01; H, 8.07; N, 10.19.

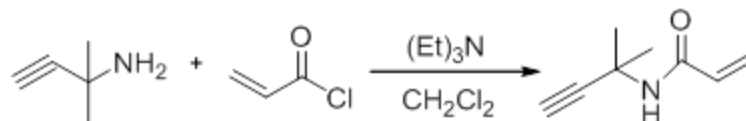


Figure 3-1 Chemical synthesis of MBAA

3.2.2 SYNTHESIS OF N- CHLORAMINE PRECURSOR

Anhydrous K₂CO₃ (10 g, 75 mmol) was added to the solution of 5, 5-dimethyldantoin (3.2 g, 25 mmol) in Me₂CO (120 mL). This suspension was heated to reflux for 0.5 h and 1,3-dibromopropane (2.8 mL, 27 mmol) was added. The mixture was allowed to reflux overnight and a

thin layer of silica gel was used to filter the reaction mixture. White solid was obtained by evaporating the filtrate and it was further purified by column chromatography (EtOAc/Hexanes=1/2-1/1) to afford bromide compound as white solid. (5.1 g, 82%); ^1H NMR (CDCl_3 , 300 MHz) δ 6.07 (br, 1 H), 3.66 (t, $J=6.9$ Hz, 2 H), 3.40 (t, $J=6.6$ Hz), 2.22 (m, 2 H), 1.46 (s, 6 H); ^{13}C NMR (CDCl_3 , 75 MHz) δ 177.2, 156.2, 58.8, 37.4, 31.2, 29.6, 25.1; HRMS (MALDI-TOF) calculated for $\text{C}_8\text{H}_{14}\text{BrN}_2\text{O}_2$ $[\text{M} + \text{H}]^+$: 249.0238, found: 249.0235.

Sodium azide (0.96 g, 14.7 mmol) was added to the bromide compound (2.4 g, 9.8 mmol) solution in DMF (20 mL). The mixture was heated to 80°C and stirred overnight. The mixture was allowed to cool and it was partitioned between EtOAc and H_2O . The organic layer was concentrated the second time to give the crude compound which was further purified using column chromatography (EtOAc/Hexanes = 1/2-1/1) to afford azido hydantoin analogue as colorless viscous oil⁷² as shown in Figure 3-2. ^1H NMR (CDCl_3 , 300 MHz) δ 6.07 (br, 1 H), 3.66 (t, $J=6.8$ Hz, 2 H), 3.40 (t, $J=6.6$ Hz), 2.22 (m, 2 H), 1.46 (s, 6 H); ^{13}C NMR (CDCl_3 , 75 MHz) δ 177.2, 156.2, 58.8, 49.1, 36.2, 27.5, 25.1; HRMS (MALDI-TOF) calculated for $\text{C}_8\text{H}_{13}\text{N}_5\text{O}_2\text{Na}$ $[\text{M} + \text{Na}]^+$: 234.0961, found: 234.0934

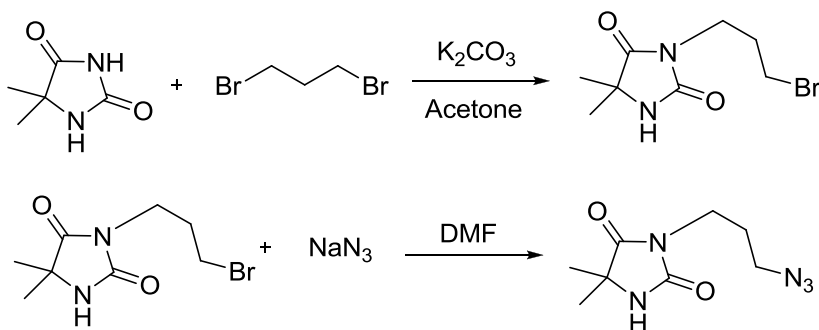


Figure 3-2 Chemical synthesis of azido-hydantoin analogue

3.2.3 SYNTHESIS OF QUATERNARY AMMONIUM COMPOUND

2-azido-N, N-dimethylethanamine (EtAm) was prepared by dissolving 69 mmol of N,N-dimethylethylamine-hydrochloride in water followed by addition of 139 mmol of sodium azide to the solution and reaction continued overnight at reflux. KOH (10 g) was added to the mixture to neutralize the residual acid and product was extracted from water by DCM after solvent evaporation. In the second stage, 21.9 mmol of EtAm was dissolved in 20 ml acetonitrile and 43.8 mmol of Iodomethane was added to the solution and reaction continued overnight at 50°C. Purification was done by adding ethyl acetate to the mixture and passed through ion-exchange resin. The synthesis reaction is shown in Figure 3-3

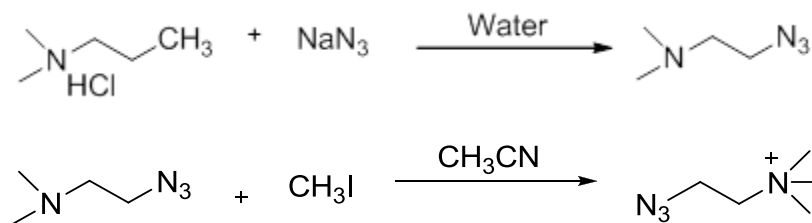


Figure 3-3 Chemical synthesis of QAC

3.3 SURFACE MODIFICATION OF PET: SEMI-INTERPENETRATING NETWORK

A successful method has been developed in “Biomaterials synthesis and surface engineering lab” to create semi-IPN on polyester fabric resulting in PET-PMBAA. A piece of cleaned PET fabrics was soaked in 20 mL methanol solution of 5.43 g (2 mol/L) MBAA monomer, 130 mg (0.045 mol/L) MBA crosslinker and 290 mg (0.082 mol/L) of Benzophenone initiator in 40°C shaking bath for 2 h. Fabrics was exposed to UV induced polymerization for 2 hrs. Afterwards,

fabric was rinsed 3-4 times with methanol and dried using vacuum oven. Then samples was weighted and IP was calculated⁷².

The immobilization percentage (IP) was calculated as follows:

$$IP = (W_2 - W_1)/W_1 \times 100$$

Where W_1 is the weight of pristine PET; W_2 is the weight of PMBAAPET

3.4 SURFACE MODIFICATION OF PET: PLASMA TECHNIQUE

An alternative method has been employed in the current study to modify the pet surface by treatment with propargyl acrylate using plasma pre-treatment followed by UV irradiation to deposit alkynyl functional groups on substrate resulting in PET-PA. A piece of pet fabric (4x3inch²) was exposed to oxygen plasma at a flow rate of 24-26 sccm for 12 min on each side. Prior to UV irradiation, fabric was placed on a glass plate and 6 ml propargyl acrylate (PA) monomer was added on the top of plasma treated fabric. A second glass plate was carefully placed on top of wet fabric in a way that fabric was sandwiched between two glass plates. PA was exposed to UV irradiation using Intelli ray 400 for 60 min.

The immobilization percentage (IP) was calculated as follows:

$$(W_2 - W_1)/W_1 \times 100$$

Where W_1 is the weight of pristine pet; W_2 is the weight of PA-treated fabric

3.5 “CLICK” REACTION BETWEEN PET-PMBAA OR PET-PA AND AZIDO MOIETIES

N-chloramine (AzH) and QAS (the amount was calculated based on active alkyne groups measured by weight increase and click reaction) and 50 mL Triton X-100 were dissolved in 20 mL

mixed solvent t-BuOH/H₂O (1:1). PET-PMBAA or PET-PA (Figure 3-4 and Figure 3-5) was immersed in this mixed solvent for 30 min before Na ascorbate (50 mol% of Azide) and aqueous CuSO₄ (10 mol% of Azide) were added to initiate the “click” reaction. The reaction mixture was continuously shaken for overnight at room temperature. Subsequently, the treated fabric was rinsed with deionized water and dried under vacuum for 24 h⁷². Different ratios of compound (*N*-chloramine to QAS) were used as shown in Table 3-1 (for 1 mol active alkyne groups on the surface).

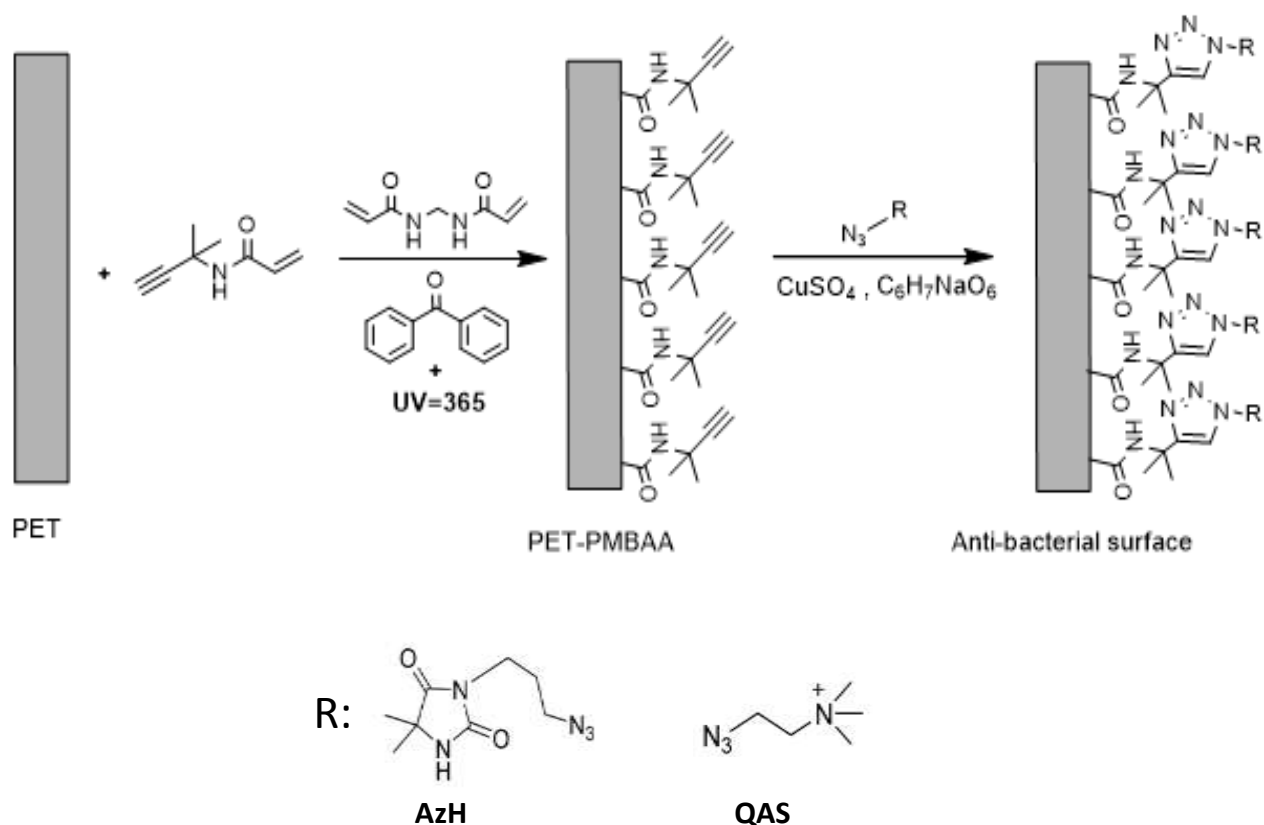


Figure 3-4. Surface modification of PET fabric using MBAA monomer to form Semi-IPN followed by click reaction using antibacterial agents

Table 3-1 Experiment design showing various ratios of Azido hydantoin and short chain QAC on the surface of fabric

Sample #	# of moles		Ratio
	Azido hydantoin	QAS	Azido hydantoin/QAS
1	0.2	0.2	50/50
2	0.2	0.467	30/70
3	0.2	0.0857	70/30
4	0.2	0	100/0
5	0	0.8	0/100

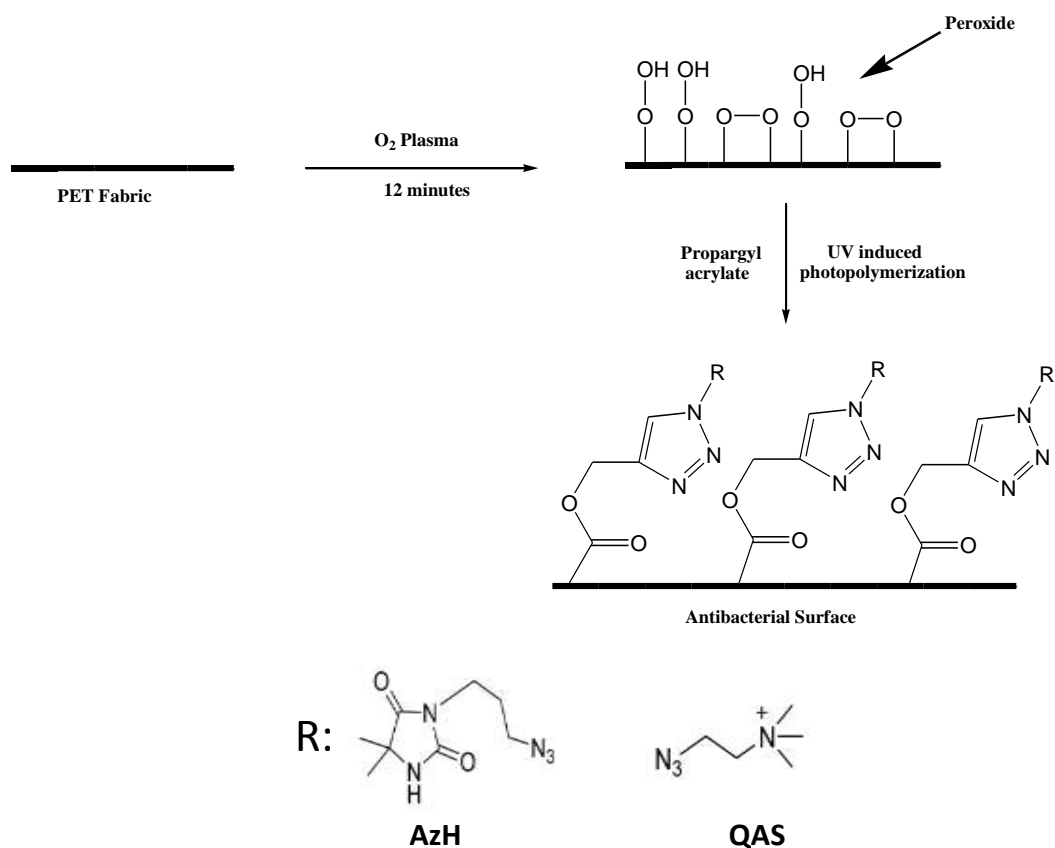


Figure 3-5 Surface modification of PET fabric using PA monomer followed by click reaction using antibacterial agents

3.6 CHLORINATION AND TITRATION OF ACTIVE CHLORINE

Chlorination of the fabric was performed with 50 mL of 1500 ppm NaClO solution. The chlorination reaction continued for 1 hr at room temperature. Aniodometric titration method will be adopted to quantify the active chlorine on the samples⁷⁴. The minimum weight of fabric sample should be 0.26–0.27 g and cut the fabric into small pieces. Add 25 ml of 0.001N sodium thiosulfate solution and shake for 30 min. The excess amount of sodium thiosulfate in the mixture was titrated with 0.001N iodine solution by monitoring milli volt changes with a redox platinum electrode. The active chlorine content of the treated PET samples was calculated from the following equation:

Active chlorine concentration [Cl+] ppm

$$[\text{Cl}+] \% = \frac{35.45}{2} \times \frac{(V_{Cl} - V_o) \times 10^{-3} \times N}{W_{Cl}} \times 100$$

V_o - control reading, V_{Cl} – Burette reading (volume of KI consumed), W_{Cl} - weight of fabric used for titration, N – normality of solution

3.7 ANTIBACTERIAL ASSESSMENT OF MODIFIED PET

“Sandwich test” was used for antibacterial assessment and the treated fabric surface were challenged with *S. aureus* and *E. coli*⁸⁴. Bacteria was suspended in pH 7, 900 μM phosphate buffer, and 100 μL of the bacterial suspensions were added to the center of two pieces of 1 inch square polyester swatches held in place by sterile weights. The sandwiched samples were tested for varying contact time points. The samples were then quenched with 5 ml of sterile 0.02N sodium thiosulfate solution to remove all oxidative chlorine, vortexed for 2 minutes and ultrasonication for 1 minute. Serial dilutions of the solutions of vortexed bacteria were made using pH 7, 900 μM

phosphate buffer, and plated on trypticase soy agar. The plates were incubated at 37⁰C for 24 h, and viable bacterial colonies are recorded for biocidal efficacy analysis.

$$\text{Percentage reduction of bacteria (\%)} = (C - D)/C \times 100$$

$$\text{Log reduction} = \text{Log} (C/D) \text{ if } D > 0; = \text{Log}(C) \text{ if } D = 0$$

Where, C is the number of bacteria counted from bleached untreated cotton, and D is the number of bacteria counted from treated fabric surface.

3.8 ZETA POTENTIAL

Zeta potential of modified PET samples loaded with azido hydantoin analogue and QAC was determined using SurPASS-Electrokinetic Analyzer having and a flat-plate measuring cell of dimension 55mm×25 mm. The analyzer performs pH titration at room temperature from pH 3 to 11 using a 1mM KCl electrolyte solution with a target ramp pressure of 300 mbar. The pH of solution was adjusted by adding 0.05 M NaOH or HCl. Zeta potentials were calculated from the streaming potentials using the Fairbrother–Mastin (F–M) equation^{85,86}.

$$\left(\frac{\Delta\varphi}{\Delta P}\right) = \zeta \frac{\epsilon_o \epsilon_r}{\eta \lambda_o} \left(\frac{\lambda_h R_h}{R}\right)$$

Here $\Delta\varphi$ is the electrical potential in the flow cell, ΔP is the applied pressure in the cell used to force the electrolyte to flow over the charged surfaces, ϵ_o is the vacuum permittivity, ϵ_r is the relative dielectric constant of the electrolyte solvent, ζ is the zeta potential, η is the dynamic viscosity of the electrolyte, λ_o is the bulk conductivity of the circulating electrolyte, λ_h is the electrical conductivity of the highly saline reference solution (100mM KCl), R_h is the measured

electrical resistance across the flow channel filled with the highly saline reference solution, and R is the measured electrical resistance across the flow channel filled with the normal experimental electrolyte.

3.9 DETERMINATION OF POSITIVE CHARGE ON THE SURFACE OF FABRIC

The positive charge on the surface of fabric can be measured using a method mentioned in 2.4.2a section. Also, we have developed another method to quantify positive charge using 4-(phenylazo) benzoic acid dye which is a pH sensitive dye as shown in Figure 3-6.

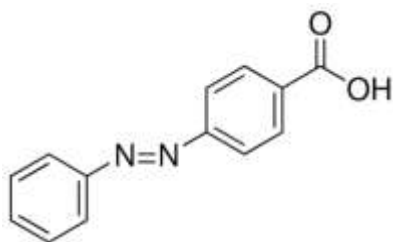


Figure 3-6 Structure of 4-(phenylazo) benzoic acid dye

Four centrifuge tubes each containing 10 mg dye dissolved in 20mL total solution (5mL water + 5mL DMSO) at pH 9 were prepared for four types of samples. The Fabric sample (25.4 x 25.4mm²) was immersed in each tube. The samples were kept in dye solution on shaker for 1 hour. The samples were washed with water and DMSO at pH 9 to remove any unfixed dye in separate centrifuge tube. The samples were then washed in mixed solution of water and DMSO at pH 3 so that the dye can detach itself completely and hence the dye which gets detached in solution can be used to quantify positive charge. The calibration curve is shown in Figure 3-7Figure 4-7

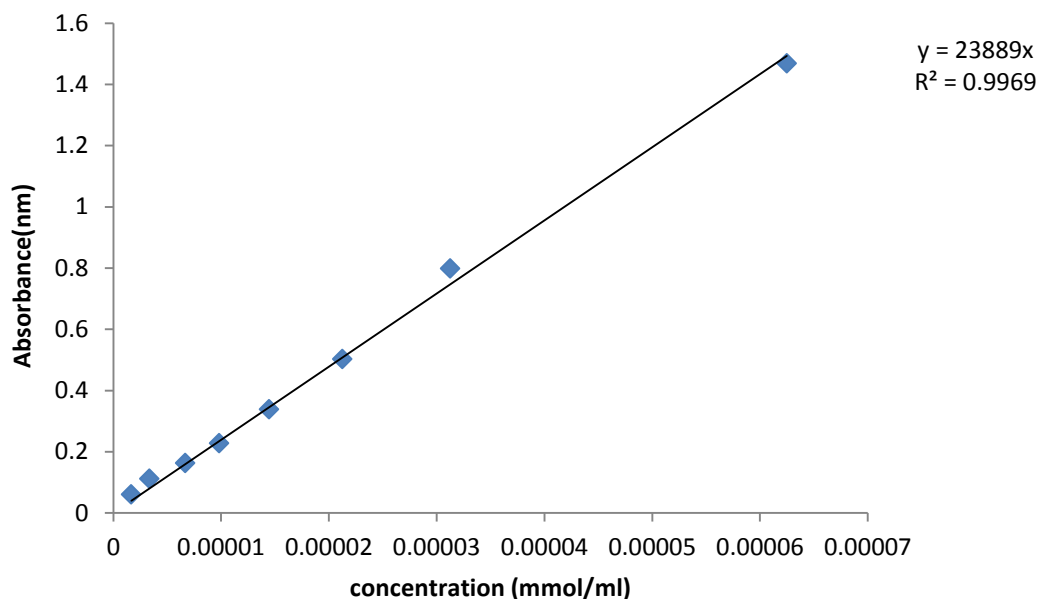
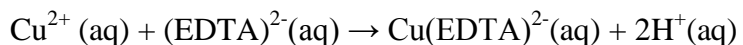


Figure 3-7 Calibration curve of 4-(phenylazo) benzoic acid dye

3.10 REMOVAL OF COPPER FROM CLICKED PET FABRIC

It has been observed that traces of copper remain on the fabric even after thorough washing of samples containing higher amount of quaternary ammonium compound (50/50 and 30/70 azido hydantoin/QAS). Unchlorinated PMBAA-clicked samples were quenched with sodium thiosulfate and titrated against iodine solution. It was observed that 224 ppm of copper existed in the samples. Copper can be removed by washing the treated samples with Ethylenediaminetetraacetic acid (EDTA). EDTA is a well-known chelating agent i.e., its ability to "sequester" metal ions such as Ca^{2+} and Fe^{3+} .



The samples were washed with EDTA for 10 min on shaker followed by washing with water. This process was repeated three times and hence complete removal of copper was observed.

4 RESULTS AND DISCUSSION

4.1 PART 1: CYCLIC AND ACYCLIC N-H GROUPS IMMOBILIZED TOGETHER ON PET SURFACE: A MIXED SYSTEM

The surface of PET fabric was modified in order to generate clickable alkynyl handles by forming three dimensional interpenetrating network (IPN) on PET surface. The IPN formation on PET surface involved photo-initiated copolymerization of amide monomer MBAA with divinyl crosslinker N,N'-methylenebisacrylamide (MBA) resulting in PET-PMBAA surface. An Azido hydantoin analogue (AzH) which acts as an *N*-chloramine precursor (3-(3-azidopropyl)-5,5-dimethylimidazolidine-2,4-dione) and an azido QAS (2-azido-N, N, N-trimethylethyl-1-ammonium chloride) were immobilized in various ratios on PET-PMBAA surface via click reactions as shown in Figure 4-1. There were two types of N-Hs on the modified PET surface: (1) N-H groups generated on the surface by cyclic AzH (2) N-H groups generated by MBAA which act as acyclic *N*-chloramine precursor. In this section, contribution of positive charge towards active chlorine loading and antibacterial efficacy of PET-PMBAA bearing AzH and QAS (PET-PMBAA-AzH/QAS) will be discussed. Majorly three types of ratios were prepared by clicking *N*-chloramine and QAC on PET-PMBAA surface: 70/30 AzH/QAS, 50/50 AzH/QAS and 30/70 AzH/QAS where 70/30 AzH/QAS refers to theoretically 70% of total clickable sites loaded with AzH and corresponding 30% sites clicked with QAS on PET-PMBAA surface. Similarly 50/50 AzH/QAS and 30/70AzH/QAS were immobilized on PET surface.

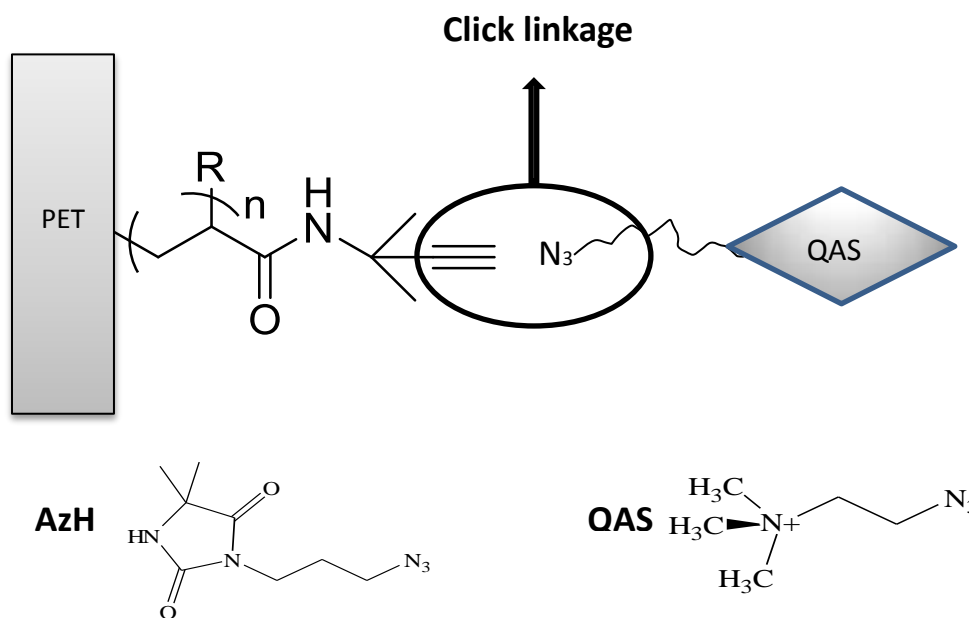


Figure 4-1 Click reaction on PET-PMBAA surface with azido hydantoin analogue and QAS

4.1.1 CONTRIBUTION OF POSITIVE CHARGE TOWARDS ACTIVE CHLORINE LOADING

An experiment was conducted to analyze the contribution of QAS towards active chlorine loading where AzH and QAS were immobilized on PET-PMBAA surface following a two-step click reaction. In the first step, same amount of AzH (0.13mmol) was clicked resulting in PET-PMBA-AzH followed by chlorination and active chlorine content was determined using iodometric titration. In the second step, varying amounts of QAS were clicked on the PET-PMBAA-AzH surface resulting in PET-PMBAA-AzH/QAS. The dosage ratios used for this experiment were 70/30 AzH/QAS, 50/50 AzH/QAS and 30/70 AzH/QAS where 70/30 AzH/QAS refers to 0.13mmol azido hydantoin clicked on surface (amount of AzH was kept constant for all the three ratios only for this experiment) and corresponding 30% sites clicked with QAS on PET-PMBAA surface.

Similarly 50/50 AzH/QAS and 30/70AzH/QAS were immobilized on PET surface. In addition to these samples, PET-PMBAA was immobilized with 100% QAS without addition of AzH (0/100 Az-H/QAS)

Table 4-1 Active chlorine loading on PET-PMBAA -AzH surface after clicking QAS in various ratios.

Sample	PET-PMBAA -AzH Active chlorine (ppm)	PET-PMBAA-AzH/QAS Active chlorine (ppm)
70/30 AzH/QAS	184	315
50/50 AzH /QAS	170	585
30/70 AzH/QAS	177	860
0/100 AzH/QAS	68	732

- Available chlorine – 1500 ppm, duration 1 hour, pH-8, additive- 1M NaCl

Table 4-2 Contribution of cyclic N-H groups towards active chlorine loading in the mixed system

Modified PET	0/70 AzH/QAS (Acyclic N-H & QAS)	30/0 AzH/QAS (Cyclic + Acyclic N-H)	30/70 AzH/QAS Cyclic + Acyclic N-H &QAS)
Active chlorine loading(ppm)	701± 28 ppm	133±5 ppm	835± 24 ppm

- Available chlorine – 1500 ppm, duration 1 hour, pH-8, additive- 1M NaCl

Chlorination of PET-PMBAA-AzH/QAS samples was performed for 1 h in a pH 8 chlorinating solution containing 1500 ppm available chlorine of the sodium hypochlorite and 1M NaCl. Active chlorine loading on PET-PMBAA-AzH surface increased after clicking QAS as shown in Table 4-1. As the amount of QAS increased on PET-PMBAA-AzH surface, active chlorine loading also increased presenting approximately 5 times for 30/70 AzH/QAS followed by 3 times for 50/50 AzH/QAS and nearly twice for 70/30 AzH/QAS as compared to the sample

without QAS. It is clear evidence of increase in active chlorine loading upon introduction of positive charges on PET-PMBAA-AzH surface and also indicates successful click reaction on the surface. Positive charge contributed to converting higher amount of N-H groups on surface to N-Cl. PET-PMBAA 0/100 AzH/QAS surface containing acyclic N-H groups showed 68 ppm active chlorine loading without the presence of AzH compound which confirmed that acyclic N-H got converted to N-Cl. The active chlorine loading was significantly enhanced to 732 ppm upon the addition of QAS which reveals that positive charge could facilitate the conversion of sterically hindered and less accessible acyclic N-H groups to N-Cl. In addition to the above findings, it has also been observed that enhanced active chlorine on the PET-PMBAA surface clicked with higher amount of QAS i.e.30/70 AzH/QAS is majorly attributed to the conversion of acyclic N-H groups to N-Cl as shown in Table 4-2. The PET-PMBAA surface bearing 0/70 AzH /QAS achieved 700 ppm active chlorine loading upon chlorination while 30/70 AzH/QAS showed 835 ppm active chlorine on surface. It means 135 ppm which amounts to only 16% of total active chlorine loading (835 ppm) on PET-PMBAA-30/70 AzH /QAS is contributed by cyclic N-H groups. Therefore, these results serve as evidence that enhanced active chlorine loading due to introduction of positive charge is majorly contributed due to higher conversion of acyclic N-H groups (700 ppm out of 835 ppm) on the PET-PMBAA surface.

Chlorination progress versus available chlorine has not been studied for PET in any of the previous publications, although similar study has been performed on cotton substrate³¹. PET is considered to be more user friendly in terms of rechargeability and physical properties such as tensile strength. High tensile strength of PET makes it more durable towards washing which is essential for recharging process and these properties make PET an appropriate choice for preparing medical textiles. Although synthetic fibers are known to have poor adsorbing property, significant

growth of bacterial species such as *Micrococcus*, *Enhydrobacter* and *Staphylococcus epidermidis* was observed on polyester T-shirts⁸⁷. Antibacterial treatment of PET based textile materials is necessary to minimize cross-contamination and outbreak of bacterial infection.

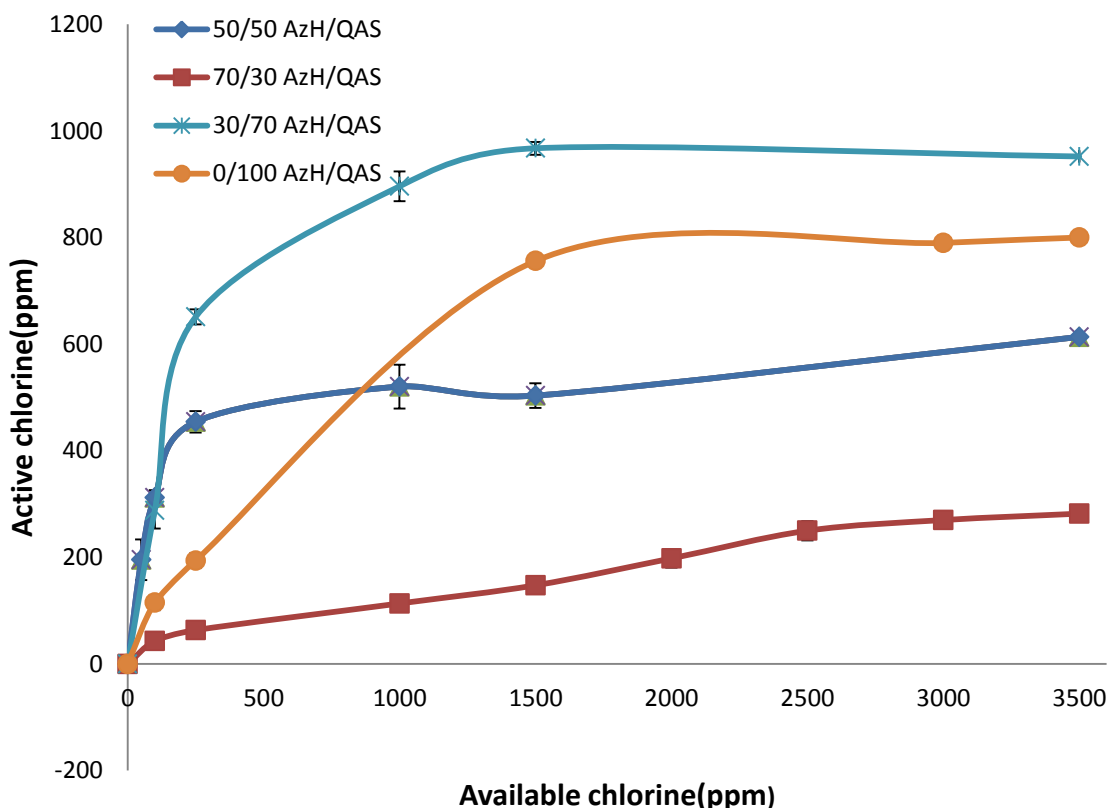


Figure 4-2 Chlorination progress versus available chlorine in NaClO solution

• Available chlorine – 100 to 3500 ppm, duration 1 hour, pH-8, additive- 1M NaCl

Figure 4-2 shows active chlorine loading on PET-PMBAA surface clicked with 70/30, 50/50 and 30/70 AzH/QAS as a function of available chlorine concentration in chlorinating solution. Chlorination of samples was performed at various levels of available chlorine with addition of 1M NaCl at pH 8 for 1 hour. The active chlorine loading on the surface increased as the amount of QAS clicked on the surfaces increased which shows contribution of positive charge towards enhanced active chlorine loading. The sequence of equilibrium active chlorine loading was: 30/70 AzH/QAS

> 50/50 AzH/QAS > 70/30 AzH/QAS. The active chlorine loadings on 30/70 AzH/QAS and 50/50 AzH/QAS were higher than 70/30 AzH/QAS over full range of available chlorine. Moreover, the active chlorine loading on 30/70 AzH/QAS increased at least by half that of 50/50 AzH/QAS and more than double of 70/30 AzH/QAS when available chlorine was above 500 ppm. Since PET-PMBAA-50/50 AzH/QAS and 30/70 AzH/QAS shows significant change in active chlorine loading when available chlorine in chlorinating solution was increased, this study also confirms that the introduction of positive charge contributed to reducing the levels of free/available chlorine used in chlorinating solutions. Interestingly, 50/50 AzH/QAS readily achieved 50% of the saturated active chlorine loading (312 ppm out of 613 ppm) at 100 ppm available chlorine. However, 30/70 AzH/QAS was loaded with 30% of the saturated active chlorine content (288 ppm out of 952 ppm) and 15 % for 70/30 AzH/QAS (43 ppm out of 282 ppm) at 100 ppm available chlorine concentration. The surface bound N-Hs of 50/50 AzH/QAS are the easiest to convert to N-Cl among all the clicked PET-PMBAA samples and this sample holds industrial importance. The highest active chlorine loading on surface was observed for 30/70 AzH/QAS at highest level of available chlorine tested. The data shows that inclusion of positive charge contributed to both faster chlorination and higher active chlorine loading. Similar to the results shown in Table 4-1, significant amount of active chlorine loading was observed on 0/100 AzH/QAS where cyclic N-H groups were not present. Moreover, higher equilibrium active chlorine on 30/70 AzH/QAS (952ppm) surface as compared to 0/100AzH/QAS(800) is due to conversion of both cyclic N-H and acyclic N-H groups with the aid of positive charge.

4.1.2 CONTRIBUTION OF POSITIVE CHARGE TOWARDS ANTIBACTERIAL EFFICACY

Effect of positive charge on the antibacterial efficacy of the surface bound *N*-chloramine was also studied. Firstly, the antibacterial efficacy of PET-PMBAA-AzH surface with and without positive charge against CA-MRSA and *E.coli* is presented in Table 4-3 and Table 4-4. In the second part of this section, comparison of the antibacterial efficacy of PET-PMBAA surface clicked with varying ratios of AzH and QAS against both gram negative and gram positive bacteria was conducted.

Table 4-3 Antibacterial results of 70/30 AzH/QAS and 70/0 AzH/QAS treated PET samples against CA-MRSA

Modified PET Samples Chlorinated	Active Chlorine (ppm) \pm STD	Available chlorine used for chlorination (ppm)	Different Contact Time(min)				
			5 min	10 min	15min	30 min	
			Percent reduction	Percent reduction	Percent reduction	Percent reduction	Log reduction
70/30 AzH/Q AS	299 \pm 5	3500	60.01	71.41	89.21	100	5.8
70/0 AzH/QAS	298 \pm 10	3500	15.15	16.67	75.81	94.73	1.27

•Inoculum concentration- 8×10^6 CFU/ml, chlorination duration 1 hour, pH-8, additive- 1M NaCl

At similar levels of active chlorine loading, PET-PMBAA surface loaded with 70/30 AzH/QAS presented 100% reduction of CA-MRSA and MDR-*E.coli* (5.8 and 5.4 log reduction, respectively) in 30 minutes. In comparison, PET-PMBAA-70/0 AzH/QAS showed 1.2 and 3.2 log reduction of CA-MRSA and MDR-*E.coli* respectively in 30 minutes. PET-PMBAA sample containing 70/30 AzH/QAS killed both MDR-*E.coli* and CA-MRSA faster and more efficiently as compared to PET-PMBAA without QAS (70/0 AzH/QAS) at similar level of active chlorine

loading as shown in Table 4-3 and Table 4-4. It was found that difference in antibacterial efficacy between samples clicked with and without QAS was considerable as well as distinguishable even after long contact time i.e. 30 minutes for CA-MRSA and *E.coli*. Active chlorine loading for samples with and without positive charge in Table 4-3 and Table 4-4 did not show significance difference ($p>0.05, n=3$). This experiment confirmed that positive charge contributed to faster killing of bacteria majorly due to electrostatic interaction between cationic charge and negatively charged cell wall of bacteria. This interaction results in active chlorine transfer from *N*-chloramine into bacterial cells which attack many vitally important constituents (such as enzymes) and denature proteins leading to cell death³¹

Table 4-4 Antibacterial results of 70/30 AzH/QAS and 70/0 AzH/QAS treated samples against MDR-*E.Coli*

Modified PET Samples Chlorinated	Active Chlorine (ppm) \pm STD	Available chlorine used for chlorination (ppm)	Different Contact Time(min)					
			10 min	20 min	30min	60 min		
			Percent reduction	Percent reduction	Log reduction	Percent reduction	Log reduction	Percent reduction
70/30 AzH/Q AS	149 \pm 0	1500	84	100	3.67	100	5.44	100
70/0 AzH/QAS	146 \pm 14	1500	24.6	76.7	0.63	100	3.27	100

• Inoculum concentration- 3.1×10^6 CFU/mL, chlorination duration 1 hour, pH-8, additive- 1M NaCl

In another set of experiment, PET-PMBAA was loaded with various ratios of *N*-chloramine and QAS: 70/30 AzH/QAS, 50/50 AzH/QAS, 70/30 and 30/70 AzH/QAS. Antibacterial efficacy of these samples activated by the chlorinating solution with the same available chlorine concentration was evaluated against CA- MRSA as shown in Table 4-5. This comparison is of industrial importance. Within 10 minutes of contact, 30/70AzH/QAS and 50/50AzH/QAS killed 100% bacteria whereas 70/30 AzH/QAS showed only 42% of reduction. It means that bactericidal

property of samples increased with increase in the amount of positive charge on the PET-PMBAA surface when all these samples were chlorinated at the same level of available chlorine. The active chlorine loadings were significantly different ($p < 0.05$, $n=3$) for three types of samples in Table 4-5. However, two factors are confounded here: contribution of positive charge to chlorination and to antibacterial activity. So, to isolate the contribution of positive charge to antibacterial activity, these samples were tested at similar levels of active chlorine loading.

Table 4-5 Antibacterial efficacy of 70/30, 50/50 and 30/70 AzH/QAS samples against CA- MRSA

Modified PET Samples Chlorinated	Active Chlorine (ppm) \pm STD	Available chlorine Used for chlorination (ppm)	Different Contact Time(min)							
			10 min		20 min		30 min		60 min	
			Percent reduction	Log reduction	Percent reduction	Log reduction	Percent reduction	Log reduction	Percent reduction	Log reduction
70/30 AzH/QAS	183 \pm 5	1500	42.6	0.24	88.6	0.94	100	5.8	100	5.8
50/50 AzH/QAS	570 \pm 10		100	5.8	100	5.8	100	5.8	100	5.8
30/70 AzH/QAS	840 \pm 5		100	5.8	100	5.8	100	5.8	100	5.8

- Inoculum concentration - 5.6×10^6 CFU/ml, chlorination duration 1 hour, pH-8, additive- 1M NaCl

Antibacterial efficacy of PET-PMBAA loaded with 70/30, 50/50 and 30/70 AzH/QAS samples was tested against MDR-*E.coli* (#70094) at similar levels of active chlorine loading as shown in Table 4-6. The active chlorine loading for all the three types of samples was not significantly different when tested among each other ($p > 0.05$, $n=2$). PET-PMBAA bearing 50/50AzH/QAS showed 5.8 log reduction in 10 minutes followed by 70/30 AzH/QAS showing 3.6 log reduction and worst efficiency for 30/70 AzH/QAS. These results indicate that sample clicked with highest amount of positive charge (30/70 AzH/QAS) did not present best antibacterial efficacy which means that biocidal efficacy of *N*-chloramine clicked surface did not increase with increase

in amount of positive charge as shown in Table 4-6. This behavior of 30/70 AzH/QAS adds another layer of complexity to the mixed system. As discussed in section 4.1, the active chlorine in the samples tested for antibacterial efficacy is composed of two types of N-Cl: acyclic and cyclic. The active chlorine loading in case of 30/70 AzH /QAS as shown in Table 4-2 was arising majorly due to higher conversion of acyclic N-H to N-Cl (700 ppm contributed by acyclic N-Cl out of 835 ppm on 30/70 AzH /QAS surface). The acyclic N-Cl is more sterically hindered and might not kill bacteria as efficiently as cyclic N-Cl present in AzH structure. The possible reason for higher conversion of acyclic N-Hs can be attributed to the covalent bonding of positive charge with MBAA resulting in close proximity of both components whereas hydantoin based cyclic N-Hs are spatially at a larger distance from positive charge which makes them less accessible for conversion. Another important finding from the results presented in Table 4-6 is that 50/50AzH/QAS surface was chlorinated using only 100 ppm available chlorine and the antibacterial efficacy was as high as 70/30AzH/QAS surface which was chlorinated using 2500 ppm available chlorine. This finding indicates that 50/50AzH/QAS holds industrial importance because it is easier to recharge and presents high antibacterial efficacy killing 100% MDR-*E.coli* in 10 minutes.

Table 4-6 Antibacterial efficacy of 70/30, 50/50 AND 30/70 AzH/QAS samples against MDR-*E.coli*

Modified PET Samples Chlorinated	Active Chlorine (ppm) \pm STD	Available chlorine used for chlorination (ppm)	Different Contact Time(min)					
			3 min	5 min	10 min	30 min		
			Percent reduction	Percent reduction	Percent reduction	Log reduction	Percent reduction	Log reduction
70/30 AzH/QAS	289 \pm 14	2500	14.3	53.4	100	3.64	100	5.85
50/50 AzH/QAS	299 \pm 9.6	100	15.3	55.3	100	5.81	100	5.85
30/70 AzH/QAS	306 \pm 9.6	120	6.1	24.3	34.1	0.18	100	5.85

- Inoculum concentration- 6.8×10^6 CFU/mL ,chlorination duration 1 hour, pH-8, additive- 1M NaCl

In this experiment plan, the complexity of mixed system due to presence of cyclic and acyclic N-H groups together on the surface was realized. It was important to isolate between cyclic & acyclic N-H groups on the surface and determine their contribution towards antibacterial efficacy in the presence of positive charge.

4.2 PART 2: CYCLIC AND ACYCLIC N-H GROUPS IMMOBILIZED SEPARATELY ON PET SURFACE

The hindrance to the understanding of the contribution of positive charge to antibacterial efficacy of cyclic and acyclic *N*-chloramines was identified. In section 4.1, it was concluded that QAS is able to significantly facilitate the conversion of acyclic N-H groups of PMBAA to N-Cl. In the combined system where both cyclic and acyclic *N*-chloramine precursors were used, it was difficult to evaluate the contribution of positive charge as well as the antibacterial efficacy of two different types of *N*-chloramine precursors. It is important to isolate each type of N-Hs and evaluate actual contribution of positive charge towards antibacterial efficacy of N-H groups of cyclic & acyclic *N*-chloramine precursor.

4.2.1 METHODS TO IMMOBILIZE CYCLIC AND ACYCLIC N-H GROUPS SEPARATELY

In the current study, two methods were used to immobilize cyclic and acyclic N-H groups separately on PET surface.

- 1 Surface modification of PET using MBAA, a monomer which can act as a source of acyclic N-H groups, followed by click reaction with QAS on PET-PMBAA surface resulting in PET-

PMBAA-QAS. This model will be used to evaluate the contribution of positive charge to antibacterial efficacy of acyclic N-H groups.

- 2 Surface modification of PET using Propargyl Acrylate (PA), a monomer which does not contain N-H groups in its structure, followed by click reaction with cyclic *N*-chloramine as well as QAS resulting in PET-PA-AzH/QAS. This model will be used to evaluate contribution of positive charge to antibacterial efficacy of cyclic N-H groups.

4.2.2 CONTRIBUTION OF POSITIVE CHARGE TO CHLORINATION OF ACYCLIC N-H GROUPS

In this section, contribution of positive charge to conversion of acyclic N-H to N-Cl will be discussed. The acyclic N-H groups were imparted by MBAA during surface modification process and these N-H groups could be converted to N-Cl with aid of positive charge as discussed in section 4.1. Since the structural design of MBAA does not contain α hydrogen unlike most of the acyclic *N*-chloramines, dehydrochlorination will not occur upon chlorination and it is expected to show good antibacterial efficacy. The current study aims to determine effectiveness of acyclic *N*-chloramine on surface with and without positive charge. PET-PMBAA samples clicked with various dosages of azido QAS is represented as PET-MBAA-x% QAS, where x is dosage percentage of QAS in solution.

An experiment was conducted to compare active chlorine loading on PET-PMBAA surface with and without positive charge. Figure 4-3 shows active chlorine loading on PET-PMBAA and PET-PMBAA-100%QAS surface at various levels of available chlorine with addition of 1M NaCl at pH 8 for 1 hour. Acyclic N-H groups present in PET-PMBAA surface were very hard to be converted to N-Cl when chlorination was performed at neutral pH. Active chlorine loading was as

low as 20 ppm when the chlorination was conducted at 1500 ppm available chlorine. In order to boost the active chlorine loading on PET-PMBAA surface, chlorination of PET-PMBAA was conducted at pH 3 by adding acetic acid which could react with hypochlorous acid to form acetyl hypochlorite (CH_3COOCl). Acetyl hypochlorite has been recognized as the strongest chlorinating agent among all the chlorinating species⁵¹. The chlorination of PET-MBAA surface conducted at pH 3 boosted the active chlorine loading on PET-PMBAA surface from 20 – 68 ppm at 1500 ppm available chlorine concentration. Results presented in Figure 4-3 demonstrated that active chlorine loading on PET-PMBAA-100%QAS surface was drastically higher than PET-PMBAA surface. PET-PMBAA surface without positive charge could achieve only 180 ppm (0.9% conversion of N-H to N-Cl) active chlorine at highest level of available chlorine tested whereas PET-MBAA-100%QAS was loaded with 800 ppm (4% conversion of N-H to N-Cl) active chlorine. There is more than threefold increase in active chlorine loading on PET-PMBAA surface after inclusion of positive charge. PET-PMBAA-100%QAS showed significant variation in active chlorine loading when available chlorine in chlorinating solution was changed as shown in Figure 4-3. Acyclic N-Hs incorporated by MBAA are relatively difficult to convert to N-Cl compared to cyclic N-Hs due to the steric hindrance of two methyl groups of MBAA. It was evident from these results that positive charge facilitated the conversion of sterically hindered acyclic N-Hs imparted on PET surface. The amount of amine groups on PET-PMBAA-x%QAS surface was determined using a colorimetric assay based on pH sensitive 4-(phenylazo) benzoic acid dye. This dye can form 1:1 complex with surface accessible quaternary amines through electrostatic bonding. The amount of dye bonded onto surface was determined using UV-vis spectroscopy as discussed in section 3.9. Moreover, characterization of PET-PMBAA-QAS surfaces was performed by analyzing zeta potential of the treated surface and chlorination kinetics.

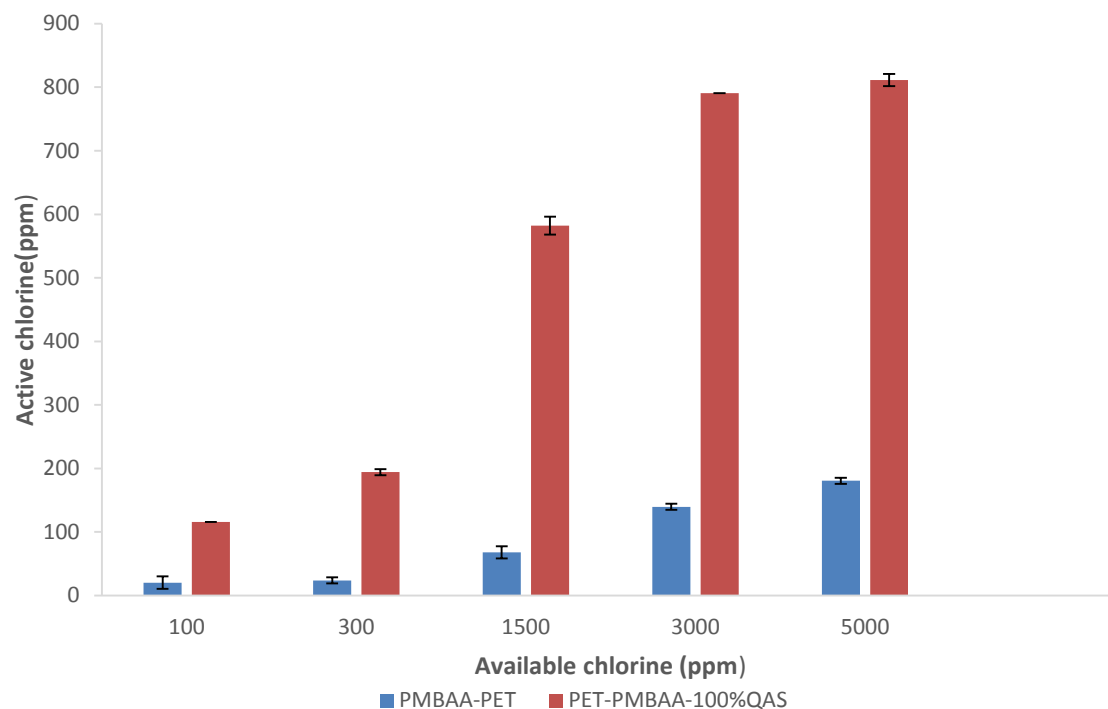


Figure 4-3 Chlorination progress versus available chlorine in NaClO solution with addition of 1M NaCl at pH 8 for 1 hour

- Available chlorine – 100 to 5000 ppm, duration 1 hour, pH-8, additive- 1M NaCl

4.2.2.1 TITRATION OF POSITIVE CHARGE ON PET-MBAA/QAS SURFACE

The positive charge on PET-PMBAA-x%QAS surface was quantified using a colorimetric method based on pH sensitive dye 4-(phenylazo) benzoic acid dye and UV-vis spectroscopy as described in section 3.9. The maximum absorbance of the pH sensitive dye was obtained at 329 nm. The dye was absorbed on positively charged PET-PMBAA surface at pH 9 and was removed from the surface at pH 3. The washed off dye from treated fabric was collected and absorbance of resultant aqueous solution was measured at 329 nm. The calibration curve was used to determine the concentration of the aqueous solution and hence the density of QAS on PET-PMBAA surface was calculated as amount of dye per unit area.

Table 4-7 QAS immobilized on PET-MBAA/QAS surface with respect to dosage percentage

Modified PET	30%QAS	50% QAS	70% QAS	100% QAS
Concentration of QAS on PET surface (mmol/cm ²)	4.72X10 ⁻⁵	7.76 X10 ⁻⁵	1.15X10 ⁻⁴	1.41 X10 ⁻⁴
% QAS immobilized on surface	1.70	2.80	4.22	5.07
Surface charge density (charges/cm ²)	2.85 x10 ¹⁶	4.68x10 ¹⁶	6.97x10 ¹⁶	8.47x10 ¹⁶

The amount of QAS added in solution during click reaction might not be the same as amount of QAS immobilized on PET-PMBAA surface. It was necessary to calculate the actual amount of QAS loaded on the PET-PMBAA/QAS surface. This quantification would help to create a baseline for minimum amount of positive charge on the surface required to contribute towards higher antibacterial efficacy as well as active chlorine loading. As shown in Table 4-7, the amount of positive charge clicked on the PET-MBAA-100% QAS surface was 1.4×10^{-4} mmol/cm² which amount to 8.47×10^{16} charges/cm². It means only 5% of the total clickable sites on PET-PMBAA surface were clicked with azido QAS whereas the amount of QAS added during click reaction was intended to cover 100% clickable sites. Similarly, the QAS (%) immobilized on PET-PMBAA surface clicked with other ratios was also calculated which amount to 1.7 % on surface for PET-PMBAA-30%QAS, 2.8% for PET-PMBAA-50%QAS and 4.22% for PET-PMBAA-70%QAS. Overall, the range of charge density on PET-PMBAA-QAS surface was ranging from 2.85×10^{16} – 8.47×10^{16} charges/cm² and the actual clickable sites available for QAS click varied from 1.7 to 5% on PET-PMBAA surface.

Titration of positive charge on PET-PMBAA-QAS surfaces revealed the amount of amine groups on PET surface and this data is used as a reference point to represent PET-PMBAA-x%QAS in the characterization methods discussed in the below sections. There is yet another way to study the surface charge characteristics by determining zeta potential of the positively charged surface.

4.2.2.2 ZETA POTENTIAL VALUES FOR PET-MBAA/QAS SURFACE

Surface charge characteristics of polymeric substrates are most commonly described through zeta potential values determined from electro-kinetic measurements. In this case, zeta potential is a promising technique to study the interaction of negatively charged chlorinating species and positively charged surface at different pH conditions. The substrate acquires surface charge when brought in contact with an aqueous medium and this charge influences the distribution of ions at the polymeric substrate-solution interface where co-ions are repelled from the membrane surface while counterions are attracted to it. In the current study, zeta potential of PET-PMBAA-x% QAC surfaces was analyzed over a pH range of 3-10 as shown in Figure 4-4. As the density of positive charge on the surface increased, the isoelectric point (IEP) moved towards higher pH and IEP values for various types of modified fabric were found to be as given below:

PET-PMBAA-30%QAS – pH 6.5

PET-PMBAA-50% QAS – pH 7.5

PET-PMBAA-70% QAS – pH 8.8

PET-PMBAA-100% QAS – pH 8.5

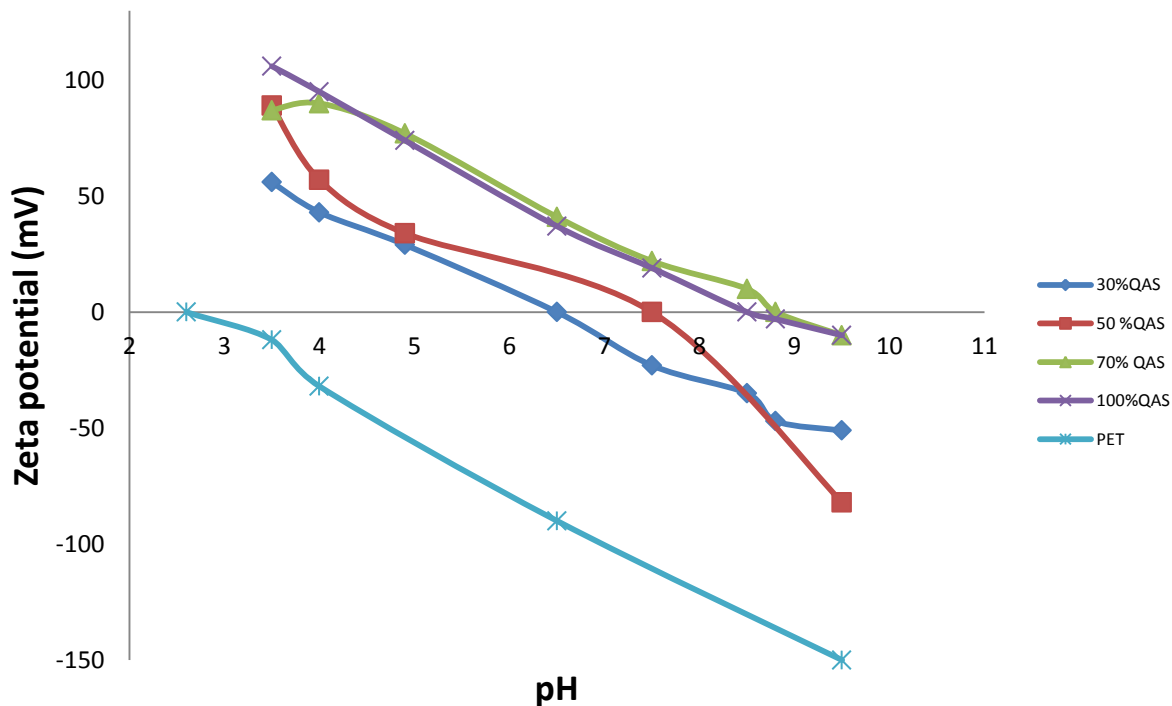


Figure 4-4 Zeta potential graph of PET-PMBAA-x%QAS samples

PET-PMBAA-x%QAS samples bear well distributed zeta potential values at pH 7.5: negative potential for PET-PMBAA-30%QAS, 50% QAS held neutral charge whereas 70 and 100% QAS presented positive charge. This pH can be selected to prepare chlorination kinetics curve. PET-PMBAA-100% QAS and 70% QAS possess higher positive zeta potential as compared to PET-PMBAA-50% QAS and 30% QAS showing that PET-PMBAA-100% QAS and 70% QAS are more positively charged than 50% and 30% QAS.

Highly negative zeta potential at basic pH on PET fabric resulted due to its hydrophobic nature. On account of the hydrophobic nature of the polyester fibres, a strong negative potential develops on its surface when immersed in aqueous solutions. In aqueous solutions, since anions are less hydrated than cations, they can more closely approach the treated surface. The surface then acquires a more negative zeta potential due to the presence of anions beyond the plane of shear. The

zeta potential graph for PET-PMBAA-x% QAS surfaces shown in Figure 4-4 presented positive surface charge in the lower pH range, passed through an isoelectric point, and then became negative in the higher pH range. This shape of the zeta potential curves is indicative of amphoteric surfaces⁸⁸. In the present case, the polyester fibres contain certain -COOH groups; as a result of presence of MBAA (which is an acrylamide), CONH incorporated in the fibre structure impart amphoteric character to the modified polyester fabric. The negative zeta potential increased with increase in pH on the alkaline side due to increased dissociation of -COOH groups. The positive potential increased with decrease in pH on acidic side due to increased protonation of -CONH groups of the MBAA monomer present on the surface.

In addition to the comparison of PET-MBAA-QAS surfaces, zeta potential values were obtained to compare PET-PMBAA-70/30AzH/QAS (mixed system) and PET-PMBAA-30%QAS as shown in Figure 4-5. Zeta potential on the surface of PET-PMBAA-70/30 AzH/QAS is lower than that on PET-PMBAA-0/30AzH/QAS in the studied full pH range. It might be because of competition between AzH and QAS towards available active sites. Also, IEP for 70/30 AzH/QAS is close to pH 4.8 whereas IEP for PET-PMBAA-30%QAS is 6.2. In nut-shell, zeta potential proved to be a useful tool to study the surface charge characteristics of PET-PMBAA-QAS samples. Based on zeta potential curve obtained for PET-PMBAA-x%QAS samples, chlorination kinetics was studied at pH value (pH 7.5) where biggest difference in zeta potential values was observed as discussed in section 4.2.2.3.

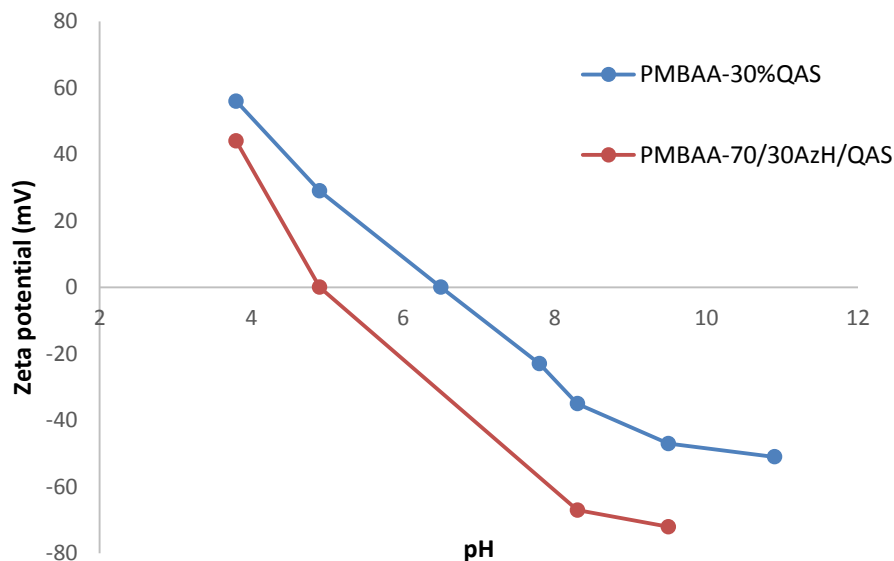


Figure 4-5 Zeta potential graph of PET-PMBAA-AzH/QAS and PET-PMBAA-QAS sample

4.2.2.3 CHLORINATION KINETICS OF PET-MBAA-QAS

Chlorination kinetics of PET-MBAA-x% QAS was studied at different time intervals in range of 5 – 120 minutes using 1500 ppm available chlorine at pH 7.5 as shown in Figure 4-6. The corresponding active chlorine content was determined till the saturation point was achieved and the rate of chlorination was determined from this study. Chlorination was performed at pH 7.5 based on zeta potential curve (Figure 4-4) which showed that at this particular pH value, isoelectric point appeared for PET-PMBAA-50% QAS treated sample, negative potential for PET-PMBAA-30% QAS treated sample and positive potential for PET-PMBAA-70% and 100% QAS treated sample. Therefore, different behaviors were expected from PET-PMBAA samples with varying ratio of QAS and the data obtained from this experiment for PET-MBAA-x% QAS was analyzed with respect to surface charge density.

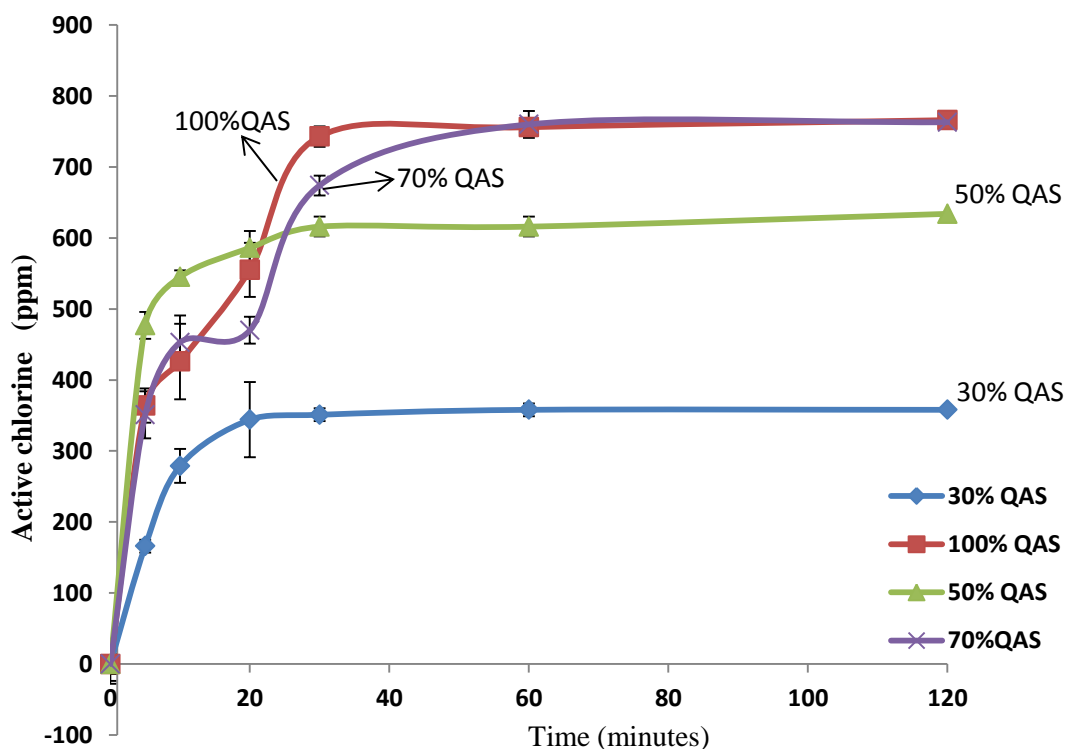


Figure 4-6 Chlorination progress Vs time for PMBAA-PET-x% QAS surface

• Available chlorine – 1500 ppm, duration 1 hour, pH-7.5, additive- 1M NaCl

Saturated active chlorine loading on PET-PMBAA-x%QAS samples followed the sequence: PET-PMBAA-100%QAS \approx PET-PMBAA-70%QAS > PET-PMBAA-50%QAS > PET-PMBAA-30%QAS. Saturated active chlorine loading on PET-PMBAA-x%QAS surfaces (Figure 4-6) and conversion ratio (%) of acyclic N-H to N-Cl was plotted as a function of surface charge density as shown in Figure 4-7. The conversion ratio of acyclic N-H to N-Cl was determined for PET-PMBAA-x%QAS based on saturated active chlorine loading presented in Figure 4-6 and moles of MBAA immobilized on PET-PMBAA surface. It was observed that PET-MBAA-30%QAS loaded with 2.85×10^{16} charges/cm² achieved 358 ppm saturated active chlorine loading compared to 616 ppm for 4.68×10^{16} charges/cm². The difference between the saturated active chlorine loadings of both the samples is significant ($p < 0.05$, $n = 3$). It means active chlorine loading on PET-MBAA surface could be increased to more than 50% when charge density of QAS increases from 2.85

$\times 10^{16}$ to 4.68×10^{16} charges/cm². As the density of positive charge on PET-PMBAA increased from 6.97×10^{16} to 8.47×10^{16} charges/cm², no further increase in saturated active chlorine loading was observed. There was no significant difference between saturated active chlorine for these surface ($p > 0.05$, $n=3$).

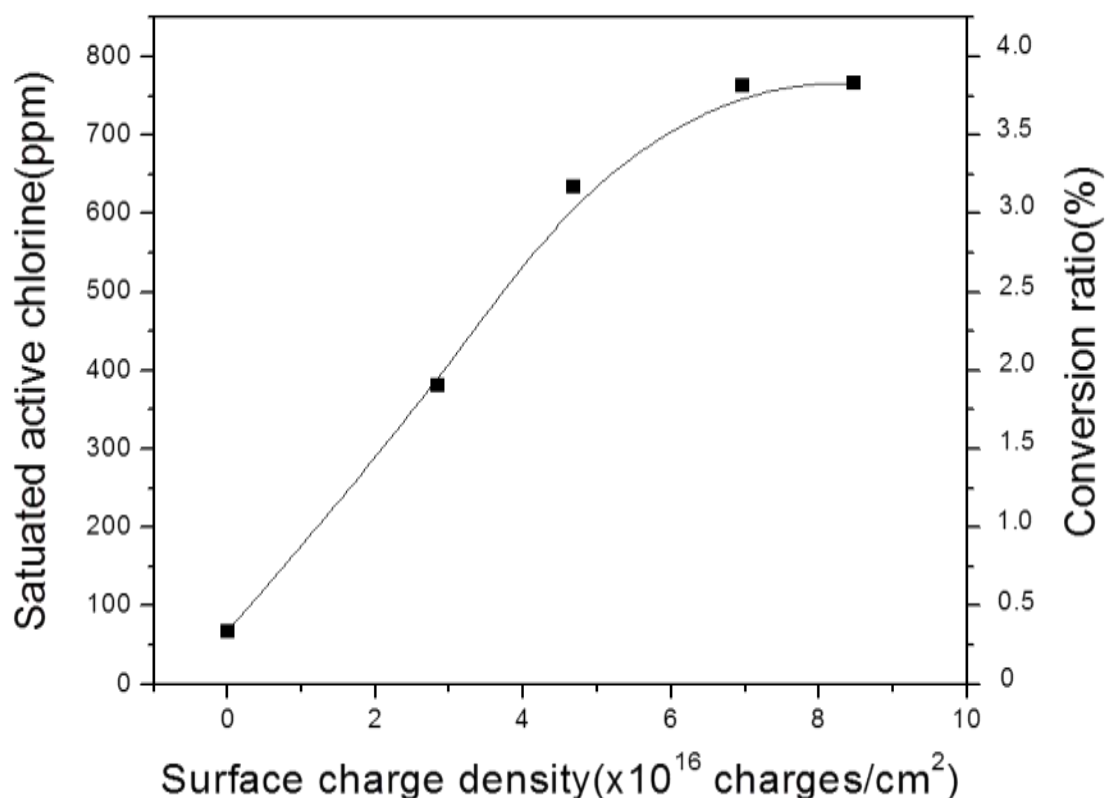


Figure 4-7 Surface charge density with respect to saturated active chlorine loading and conversion ratio

When it comes to conversion ratio of N-H to N-Cl, it was found that PET-PMBAA without positive charge showed only 0.39% conversion (based on 68ppm active chlorine on PET-PMBAA at pH 8 at 3500ppm available chlorine) whereas PET-PMBAA-70%QAS bearing positive charge density 8.4×10^{16} charges/cm² presented 3.92% conversion. It means 9 fold increase in conversion of N-H to N-Cl was obtained on surface loaded with positive charge (8.4×10^{16} charges/cm²) as

compared to PET-PMBAA without positive charge. Conversion ratio was found to be 3.90% when charge density was 6.97×10^{16} charges/cm² and further increase in positive charge density presented no significant increase in conversion ratio of N-H to N-Cl. PET-PMBAA surfaces loaded with 4.68×10^{16} and 2.85×10^{16} charges/cm² presented 3.25% and 1.95% conversion of N-H to N-Cl respectively.

The maximum conversion ratio was approximately 4% which indicates that surface interpenetrating network created on PET-PMBAA during modification PET allowed only a small fraction of accessible alkynyl groups available for click reaction. The remaining alkynyl groups were embedded in the network serving as a base foundation for the outer accessible alkynyl groups. Interestingly, this data can also be used to correlate the percentage conversion ratio of N-H to N-Cl in PET-PMBAA-QAS surface with percent immobilized alkynyl groups being clicked with QAS since available alkyne group and N-H groups available for conversion follow 1:1 ratio. As shown in Table 4-7, the percentage of QAS immobilized on PET-MBAA-x%QAS surfaces is presented which can be used to estimate number of alkynyl groups available for click reaction. If we correlate conversion ratio (%) with percentage of actual clickable sites on PET-PMBAA surface accessible for QAS click, PET-PMBAA with charge density 2.85×10^{16} possess 1.9% conversion of N-H to N-Cl and 1.7% QAS was immobilized on this surface (Table 4-7). These numbers indicate the presence of approximately same amount of N-H groups and accessible alkynyl groups on PET-MBAA surface. Similarly, PET-PMBAA with positive charge density 4.68×10^{16} showed 3.25% conversion of N-H to N-Cl and holds 2.79% QAS on surface. Similarly, correlation can be observed in other ratios as well. In addition to these observations, another important information derived from saturated active chlorine content and charge density on PET-PMBAA-x%QAS is the determination of actual ratio of N-chloramine to QAS on surface as shown in Table 4-8.

Table 4-8 Ratio of *N*-chloramine to QAS on PET-PMBAA-x%QAS surfaces

PET- PMBAA/x%QAS	30%QAS	50% QAS	70% QAS	100% QAS
<i>N</i> -chloramine:QAS on surface	26.4:10	28.5:10	23:10	19:10

In order to establish a correlation between positive charge density of PET-MBAA-x%QAS surface and chlorination kinetics, percent active chlorine obtained in 5 minutes on PET-MBAA-X%QAS samples (Figure 4-6) was plotted as a function of surface charge density of these samples (Table 4-7) as shown in Figure 4-8. Within the range of surface charge densities tested in this study, it was observed that when charge density reached 4.68×10^{16} charges/cm², 75% of the total active chlorine loading was achieved within 5 minutes of chlorination. This sample achieved highest amount of active chlorine loading in 5 minutes and reached the saturation value in least amount of time as compared to other three samples. The possible reason for such behavior could be higher accessibility of N-H groups for conversion to N-Cl when positive charge density reached 4.68×10^{16} charges/cm². This observation shows that existence of a specific charge density (in this case 4.68×10^{16} charges/cm²) can result in faster chlorination of treated fabric and holds industrial importance.

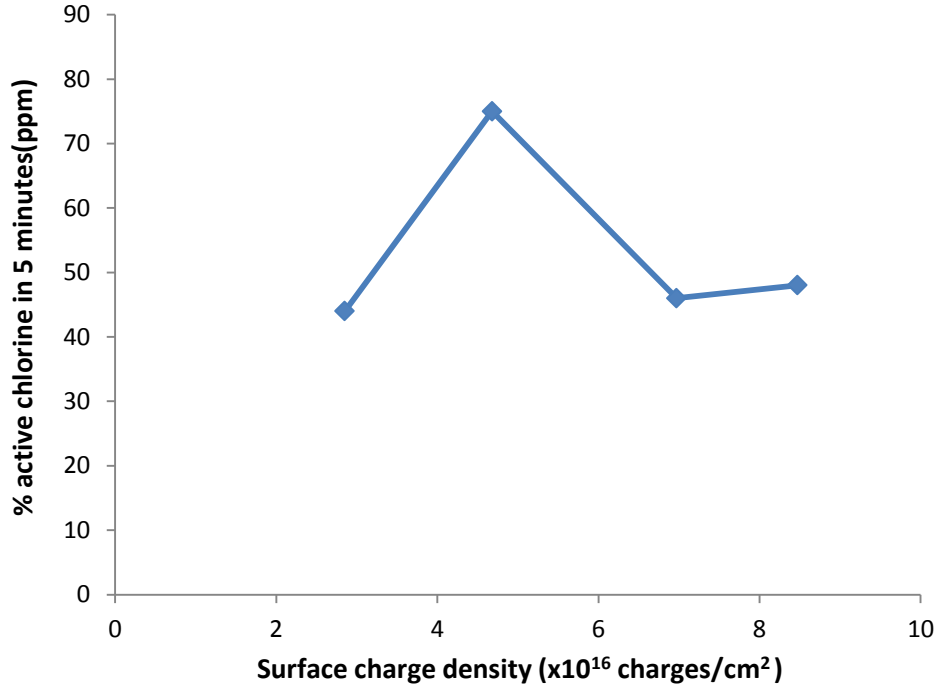


Figure 4-8 Surface charge density Vs percent active chlorine loading in 5 minutes

The chlorination reaction of *N*-chloramine could be regarded as being in first- order relationship to the concentration of amide as reported in previous studies³¹ and hence, the chlorination rate constant k was calculated based on the below equation:

$$v = d(N-Cl)/dt = k (NaClO) (amide) \quad (1)$$

$$v = d(N-Cl)/dt = k [(N-H)_0 - (N-Cl)_t] \quad (2)$$

where v is chlorination reaction rate, k is the rate constant and t is reaction duration.

Integration of equation 1 gives:

$$\ln [(N-H)_0 - (N-Cl)_t] = -k_{obs} t \quad (3)$$

where k_{obs} is observed rate constant, $[N-Cl]_t$ is *N*-chloramine concentration at reaction time and $[N-H]_0$ is total amide of MBAA on PET calculated as total IP 7.5%) As $NaClO$ was used in excess during chlorination, $k[NaClO]$ can be regarded as constant k_{obs} .

k_{obs} was calculated as shown in Figure 4-9 where total amide $[\text{N-H}]_0$ was 760ppm and $[\text{N-Cl}]_t$ was obtained from Figure 4-6. The rate constant k of PET-MBAA/QAS was calculated based on K_{obs} as shown in Table 4-9.

Table 4-9 Rate constant for the chlorination of modified PET fabric

PET- PMBAA/x%QAS	30%QAS	50% QAS	70% QAS	100% QAS
Rate constant $k[\text{L mol}^{-1} \text{s}^{-1}]$	1.08×10^{-3}	2.98×10^{-3}	2.14×10^{-3}	1.94×10^{-3}

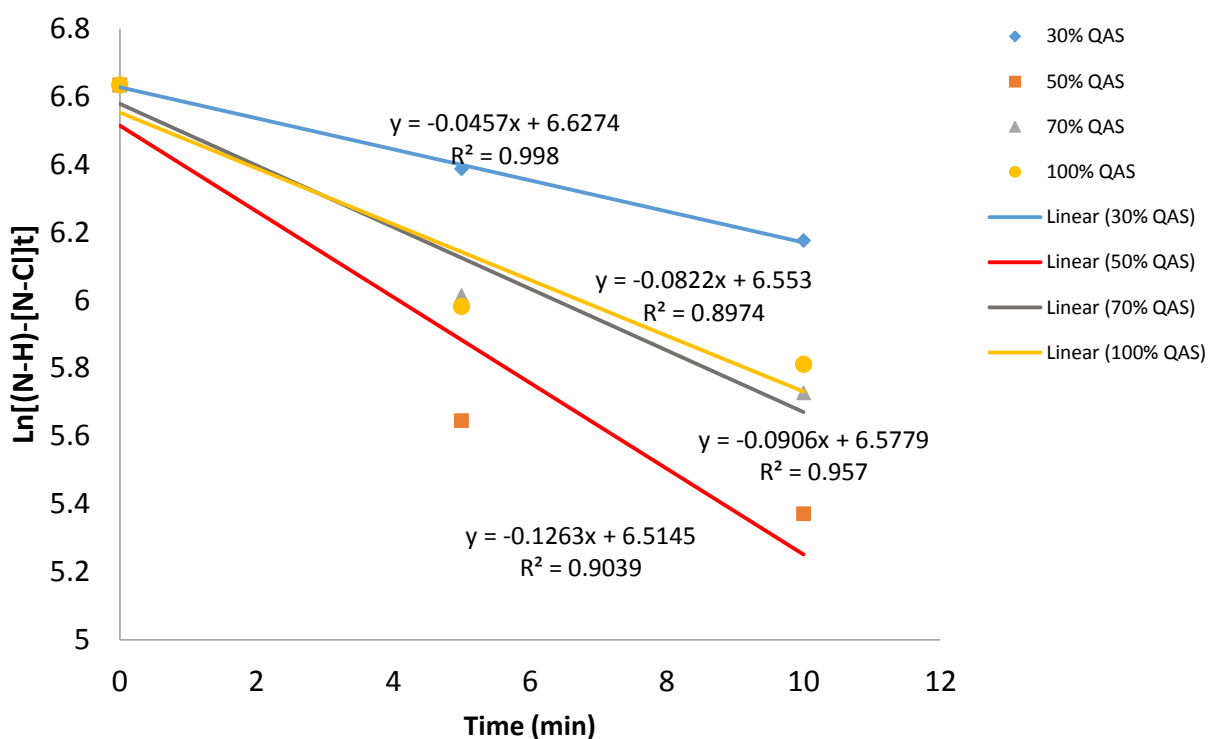


Figure 4-9 Chlorination kinetics graph showing K_{obs} for various ratios of QAS clicked on surface

Rate constant of PET-PMBAA-50%QAS representing 4.68×10^{16} charges/ cm^2 density of QAS is highest among all the modified samples which mean that chlorination of this sample

proceeds at a much faster rate compared to other three samples. Another interesting observation is that the rate constant can be increased significantly from $1.08 \text{ L mol}^{-1} \text{ s}^{-1}$ to $2.98 \text{ L mol}^{-1} \text{ s}^{-1}$ as the amount of QAS clicked on PET-PMBAA surface increase from 2.85×10^{16} (PET-PMBAA-30% QAS) to 4.68×10^{16} charges/cm² (PET-PMBAA-50% QAS).

4.2.3 ANTIBACTERIAL EFFICACY OF ACYCLIC N-H GROUPS IN THE PRESENCE OF POSITIVE CHARGE

The antibacterial efficacy of acyclic N-Cl on PET-PMBAA surface with and without positive charge was tested against CA-MRSA. The efficiency of antibacterial activity of PET-PMBAA-QAS was tested at two different levels of active chlorine loading. The antibacterial test results shown in Table 4-10 demonstrate that PET-PMBAA-100%QAS having charge density 8.47×10^{16} charges/cm² at 790 ppm active chlorine loading on surface demonstrated 100% inactivation of CA-MRSA in 60 minutes. The antibacterial activity of PET-PMBAA-100%QAS is as good as that of silver based antimicrobial dressing “Acticoat”. Acticoat is proven to be effective against a broad range of bacterial strains and fungal wound pathogens.

Table 4-10 Antibacterial assessment of PET-PMBAA-QAS against CA-MRSA

Modified PET Samples Chlorinated	Active Chlorine (ppm) \pm STD	Available chlorine used for chlorination (ppm)	Different Contact Time (min)					
			10 min	20 min	30min	60 min		
			Percent reduction	Percent reduction	Log reduction	Percent reduction	Log reduction	Percent reduction
PET-MBAA-100%QAS	184 \pm 5	230	32.7	56	0.35	61	0.40	72
PET-MBAA-100%QAS	790 \pm 0	3000	98.7	100	3.43	100	3.56	100
Acticoat			98.8	100	3.33	100	3.56	100

•Inoculum concentration- 2.5×10^6 CFU/mL, chlorination duration 1 hour, pH-8, additive- 1M NaCl

The antibacterial efficacy of PET-PMBAA-100% QAS was lower when active chlorine loading was 184 ppm. Overall, PET surface containing acyclic N-H groups and QAS were found to be effective against CA-MRSA when active chlorine content was significantly high.

The antibacterial efficacy of unchlorinated PET-PMBAA-100%QAS was tested against CA-MRSA keeping unchlorinated PET-PMBAA sample as control as shown Table 4-11. PET-PMBAA-100%QAS was loaded with charge density of 8.47×10^{16} charges/cm² which is higher than minimum cationic charge density (5×10^{15} units/cm²) reported in literature for effective killing of bacterial strains. Kugler et al⁷⁰ reported total kill of gram positive bacteria (*S. epidermidis*) in 2 hours using silica beads bearing positive charge density 5×10^{15} units/cm². Also, Murata et al⁶⁸ reported total kill of *E.coli* in 60 minutes using short chain poly(quaternary ammonium) on glass surface having positive charge density 5×10^{15} units/cm². In our case, unchlorinated PET-PMBAA-100%QAS (8.47×10^{16} charges/cm²) killed 52% bacteria in 60 minutes showing that this sample can potentially kill bacteria with the aid of positive charge

Table 4-11 Antibacterial assessment of unchlorinated PET-MBAA/100QAS against CA-MRSA

Modified PET Samples	Active Chlorine (ppm) \pm STD	Different Contact Time(min)					
		10 min		20min		60 min	
		Percent reduction	Log reduction	Percent reduction	Log reduction	Percent reduction	Log reduction
Unchlorinated PET-MBAA-100% QAS	0	23.6	0.11	19.3	0.09	52.1	0.38

•Inoculum concentration - 2.5×10^6 CFU/ml, chlorination duration 1 hour, pH-8, additive- 1M NaCl

Although the positive charge density in our sample is higher than threshold charge density suggested in literature, there are other factors which should be considered to establish a fair comparison between our sample and the surfaces mentioned in literature study. For example, activity of silica beads cannot be compared with planar fabric surface and the antibacterial test method used in literature studies (modified ASTM standard: E2149-01 and epifluorescence microscopy using fluorescent markers - LiveDead, Molecular Probes) were different from the “sandwich test” used in present study.

4.2.4 CONTRIBUTION OF POSITIVE CHARGE TO THE CONVERSION OF CYCLIC N-H GROUPS

In this section, cyclic N-H groups were immobilized on modified PET surface along with positive charge and the performance of treated surface was evaluated in terms of active chlorine loading and antibacterial efficacy. Surface of PET was modified using propargyl acrylate (PA) (Figure 4-10) instead of MBAA. Since PA does not contain N-H group in its structure, interference of acyclic N-H groups generated on surface during modification process could be avoided. PET was exposed to oxygen plasma prior to the UV irradiation of surface in the presence of PA resulting in PET-PA surface. Oxygen plasma treatment was used to generate peroxides on the surface of PET fabric, which degraded upon UV irradiation to generate radicals for surface initiated copolymerization of PA.

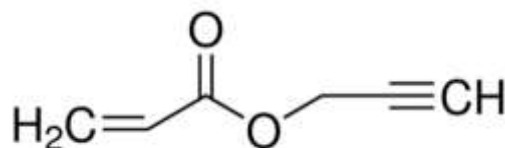


Figure 4-10 Structure of Propargyl acrylate

The weight increase after this treatment varied in the range of 2 - 3.5%. Cyclic *N*-chloramine precursor (AzH) and QAS were clicked on PET-PA surface in various ratios resulting in PET-PA- AzH/PET. The active chlorine loading with and without positive charge was determined and antibacterial efficacy of treated surfaces was compared to identify the most suitable combination of cyclic AzH and QAS on PET-PA surface.

Chlorination of PET-PA-50/50AzH/QAS and PET-PA-50/0AzH/QAS (without QAS) samples was performed at pH 8 using 100 ppm available chlorine without addition of NaCl. In this case NaCl was not added during this chlorination to avoid the interruption of NaCl which is capable of overshadowing the effect of QAS as shown in Table 4-12. Iodometric titration results demonstrated 150 ppm active chlorine loading on PET-PA- 50/50 AzH/QAS whereas only 24 ppm active chlorine was observed on sample without positive charge (50/0AzH/QAS). This amounts to fivefold increase in active chlorine loading on PET-PA-AzH surface with and without positive charge as shown in Table 4-12. Introduction of positive charge boosted the active chlorine loading on the surface.

Table 4-12 Active chlorine loading on PET-PA-AzH samples with and without positive charge

Modified PET	50/50 AzH/QAS ± STD	50/0 AzH ± STD
Active chlorine (ppm) NaCl not added during chlorination	150±19	24±14
Active chlorine (ppm) 1 M NaCl added during chlorination	136±1	120±13

• Available chlorine – 100 ppm, duration 1 hour, pH-8

The comparison of zeta potential values on PET-PA surface with and without positive charge is shown in Figure 4-11. Higher positive charge was observed in case of PET-PA- AzH/QAS as compared to PET-PA-AzH. IEP for PET-PA-AzH/QAS was 6 and that of PET-PA- AzH was observed at 4.2. The weight increase after PA treatment was in the range of 2 - 3.5% which is very less as compared to IPN treatment (7-8%). Despite of low grafting yields on PET-PA surface and subsequently limited amount of available sites for click reaction, significant amount of positive charge is presented in Figure 4-11. The possible reason could be more accessibility of alkyne groups on PET-PA surface as compared to interpenetrating network in PET-PMBAA surface where accessibility could be low due to structural hindrance.

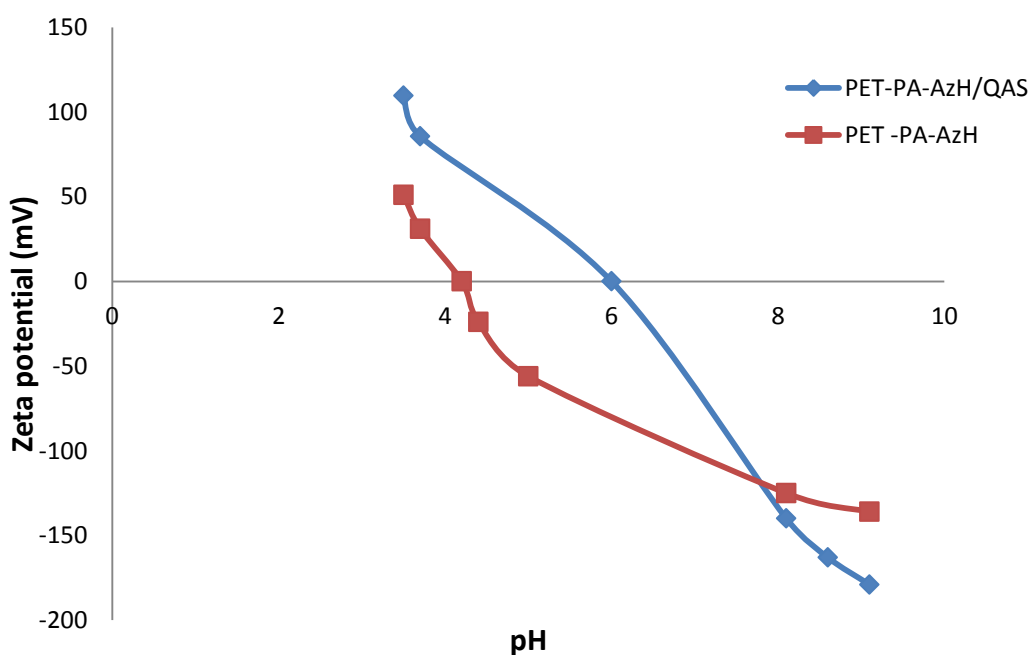


Figure 4-11 Zeta potential graph comparing PET PA-AzH/QAS and PET-PA-AzH/QAS

4.2.4.1 TITRATION OF POSITIVE CHARGE ON PET-PA-AzH/QAS

The amount of positive charge on the surface of PET-PA-AzH/QAS was calculated using a colorimetric method based on pH sensitive dye 4-(phenylazo) benzoic acid dye and UV-vis spectroscopy in the same way as mentioned in section 3.9. The dye was absorbed on positively charged PET-PA-AzH/QAS surface at pH 9 and was removed from the surface at pH 3. The dye washed off from treated fabric at pH 3 was collected and absorbance of resultant aqueous solution was measured at 329 nm. The density of QAS on treated PET surface was calculated as amount of dye per unit area. PA treated PET was not able to generate as many clickable sites as MBAA modified PET due to low grafting yield. Therefore, the concentration of QAS clicked on PET-PA surface was lower than PET-PMBAA-QAS as shown in Table 4-13. PET-PA-30/70AzH/QAS sample was loaded with 2.72×10^{16} charges/cm² which amounts to 3.89% of total clickable sites whereas PET-PA-50/50AzH/QAS and PET-PA-70/30AzH/QAS showed 2.09×10^{16} and 6.64×10^{15} charges/cm² respectively.

Table 4-13 QAC immobilized on PET-PA-AzH/QAS surface with respect to total clickable sites

Modified PET	70/30 AzH/QAS	50/50 AzH/QAS	30/70 AzH/QAS
Concentration of QAC on PET surface (mmol/cm ²)	1.10×10^{-5}	3.48×10^{-5}	4.52×10^{-5}
% QAC immobilized on surface	0.95	2.99	3.89
Surface charge density (charges/cm ²)	6.64×10^{15}	2.09×10^{16}	2.72×10^{16}

The actual ratio of *N*-chloramine to QAS on the surface of PET-PA-AzH/QAS is presented in Table 4-14 and it was determined using surface charge density and active chlorine loading on PET-PA-AzH/QAS at 1500 ppm available chlorine (pH of chlorinating solution was 8, additive-1M NaCl)

Table 4-14 Ratio of *N*-chloramine to QAS on PET-PA-AzH/QAS surface

Modified PET	70/30 AzH/QAS	50/50 AzH/QAS	30/70 AzH/QAS
<i>N</i> -chloramine:QAS on surface	75.5:10	22.8:10	17.2:10

4.2.5 CONTRIBUTION OF POSITIVE CHARGE TO ANTIBACTERIAL EFFICACY OF CYCLIC N-H GROUPS

Antibacterial efficacy of PET-PA-AzH samples against *MDR-E.coli* at similar levels of active chlorine content was determined with and without positive charge as shown in Table 4-15. The active chlorine content for 50/50 AzH/QAS and 50/0 AzH/QAS showed no significant difference ($p>0.05, n=2$). It was found that sample containing positive charge 2.09×10^{16} charges/cm² achieved 5.4 log reduction in 10 minutes compared to 3.4 log reduction in case of sample without positive charge. Since active chlorine on surface of both types of samples was similar, it was evident from the antibacterial test that introduction of positive charge contributes towards effective and faster killing of bacteria.

Table 4-15 Antibacterial test results of PET-PA 50/50 AzH/QAS and 50/0 AzH/QAS against *MDR E.coli*

Modified PET Samples Chlorinated	Active Chlorine (ppm) ± STD	Available chlorine used for chlorination (ppm)	Different Contact Time(min)							
			5 min		10 min		30 min		60 min	
			Percent reduction	Log reduction	Percent reduction	Log reduction	Percent reduction	Log reduction	Percent reduction	Log reduction
50/50 AzH/QAS	227±6	500	100	3.66	100	5.49	100	5.49	100	5.49
50/0 AzH/QAS	231±4	800	99.6	2.42	100	3.49	100	3.82	100	5.49

•Inoculum concentration - 3×10^6 CFU/ml , chlorination duration 1 hour, pH-8, additive- 1M NaCl

It was found that sample containing positive charge 2.09×10^{16} charges/cm² achieved 5.4 log reduction in 10 minutes compared to 3.4 log reduction in case of sample without positive charge. Since active chlorine on surface of both types of samples was similar, it was evident from the antibacterial test that introduction of positive charge contributes towards effective and faster killing of bacteria.

Table 4-16 Antibacterial test results of PET-PA-70/30, 50/50 AzH/QAS and 30/70 AzH/QAS against *MDR E.coli*

Modified PET Samples Chlorinated	Active Chlorine (ppm) ± STD	Available chlorine used for chlorination (ppm)	Different Contact Time(min)					
			3 min	5 min	10 min		30 min	
			Percent reduction	Percent reduction	Percent reduction	Log reduction	Percent reduction	Log reduction
70/30 AzH/QAS	231±4.9	500	6.47±2.8	59± 7.7	98.7±1.7	1.9±1.7	100±0	5.85±0
50/50 AzH/QAS	221±9	500	2.88±3.5	65.4±1.4	98.9±2.4	1.94±2.4	100±0	5.85±0
30/70 AzH/QAS	218±0	800	1.15±4.2	80.1±4.2	100±0.7	5.80±0.7	100±0	5.85±0

•Inoculum concentration - 5.7×10^6 CFU/ml , chlorination duration 1 hour, pH-8, additive- 1M NaCl

We have also shown comparison of antibacterial activity among various ratios of AzH/QAS clicked on PET-PA surface at similar level of active chlorine content to evaluate the most efficient combination on surface. The active chlorine loading of 70/30 AzH/QAS when compared to other two types of samples showed no significant difference ($p > 0.05, n=2$). Interestingly, results presented in Table 4-16 shows that PET-PA-AzH surface with highest amount of positive charge shows fastest killing of bacteria. The order of antibacterial activity follows: 30/70 AzH/QAS > 50/50 AzH/QAS \geq 70/30 AzH/QAS where 30/70 AzH/QAS (17.2:10 AzH/QAS on surface) achieved 5.80 log reduction in 10 minutes compared to 1.94 log reduction for 50/50 AzH/QAS and 1.90 log reduction for 70/30 AzH/QAS. Overall, it has been proved that introduction of positive charge helps in faster killing of bacteria and the efficacy increases as the amount of positive charge on surface increases. In this case, cyclic N-H groups were converted to N-Cl unlike mixed system where maximum conversion was achieved from acyclic N-H groups as described in section 4.1.1

5 CONCLUSIONS AND FUTURE WORK

The growing risk of cross contamination and outbreak of microbial infections in health care facilities as well as household environment has led to the development of effective antibacterial surfaces as a high research priority. The role of contaminated textile substrates in spreading microbial infection in hospital environment has long been recognized^{18,19}. Despite of the regular laundering of hospital textiles, recovery of bacterial strains from these fabrics is reported stating that *Staphylococcus aureus* survived a 10 min laundering at 54°C followed by drying⁸⁹. In order to minimize the spread of microbial infections, there is an urgent need to develop new highly effective rechargeable antibacterial surfaces. Study related to combined use of various antibacterial agents together as one “antibacterial system” is very scarce. The present study aimed to fill this major gap in literature by developing a PET surface immobilized with *N*-chloramine and short chain QAS (conferring positive charge) to study the combined effect of both the biocides and optimize the ratio of two components on the modified PET surface. The three dimensional interpenetrating network was formed on PET surface resulting in PET-PMBAA to generate alkynyl handle for easy and versatile bonding of clickable moieties. Also, an alternative approach was used to generate alkynyl handles using oxygen plasma followed by UV copolymerization of propargyl acrylate resulting in PET-PA surface. The dissertation can be divided into three parts: **1** Introducing cyclic *N*-chloramine(AzH), acyclic *N*-chloramine(MBAA) and short chain QAS together(mixed system) to determine the antibacterial efficacy as well as contribution towards active chlorine loading on PET surface **2** Attaching acyclic *N*-chloramine and QAS on PET surface **3** Attaching cyclic *N*-

chloramine and QAS on modified PET surface. The *N*-chloramine and QAC were clicked in various ratios on modified PET surface. Apart from analysing antibacterial activity and active chlorine loading, quantification of positive charge on modified PET surface was conducted to correlate surface charge density with the conversion ratio of N-H to N-Cl, chlorination kinetics as well as antibacterial activity.

In the first part of dissertation referring to a mixed system, PET surface was furnished with alkynyl handles by forming three dimensional interpenetrating network using monomer MBAA in the presence of crosslinker MBA and photo-initiator benzophenone resulting in PET-PMBAA surface. Alkynyl handles on PET-PMBAA surface were loaded with various ratios of azido based cyclic *N*-chloramine (AzH) and azido short chain QAS resulting in PET-PMBAA-AzH/QAS surface. PET-PMBAA-AzH/QAS surface is referred to as mixed system due to the presence of additional acyclic N-H groups introduced by monomer MBAA during the surface modification process. It was observed that positive charge facilitated higher conversion of both cyclic and sterically hindered acyclic N-H groups on PET-PMBAA-AzH/QAS surface. Interestingly, 84% of the total active chlorine loading on PET-PMBAA-AzH/QAS surface was contributed by the conversion of acyclic N-H to N-Cl in the mixed system. It means positive charge is very effective in facilitating the conversion of acyclic N-H which is otherwise hard to convert owing to the steric hindrance by two methyl groups. The antibacterial efficiency of PET-PMBAA-30/70AzH/QAS sample was inferior to the compounds with lower amount of QAS (50/50 AzH/QAS and 70/30AzH/QAS) at similar level of active chlorine loading. The reason for low antibacterial efficacy of this sample containing highest amount of QAS is attributed to the higher conversion of acyclic N-H groups to N-Cl than cyclic N-H groups. Killing efficiency of acyclic *N*-halamines is less active than cyclic *N*-halamines. Overall, the presence of two types of N-Hs(cyclic and acyclic)

in the mixed system makes it very complex and contribution of positive charge towards conversion of each type of N-H as well as antibacterial efficacy of converted N-Cl was hard to determine. The experiments were designed to isolate cyclic and acyclic N-Hs on the modified PET surface and their contribution in the presence of positive charge was evaluated.

In the second approach, acyclic *N*-chloramine and QAS were immobilized on PET surface (PET-PMBAA/QAS) to determine the contribution of positive charge towards conversion of acyclic N-Hs and their antibacterial efficacy. The amount of MBAA loaded on PET was kept constant for several samples and amount of QAS was varied depending on total clickable sites resulting in PET-PMBAA-30% QAS, PET-PMBAA-50% QAS, PET-PMBAA-70% QAS and PET-PMBAA-100% QAS surfaces. There was more than sevenfold increase in the active chlorine loading on PET-PMBAA-100%QAS surface as compared to PET-MBAA without positive charge at 1500 ppm available chlorine in chlorinating solution. Successful loading of QAS was evident from quantification of positive charge using pH sensitive dye showing 8.47×10^{16} charges/cm² density of QAS loaded on PET-MBAA-100% surface, 6.97×10^{16} charges/cm² on PET-PMBAA-70% QAS, 4.68×10^{16} charges/cm² on PET-PMBAA-50% QAS and 2.85×10^{16} charges/cm² on PET-PMBAA-30%QAS. Within the range of charge densities tested in the current study, fastest chlorination (within first five minutes of chlorination) occurred when the surface charge density on PET-MBAA-QAS reached 4.68×10^{16} charges/cm² and saturated active chlorine loading on PET-PMBAA surface could be increased to more than 50% when charge density of QAS increases from 2.85×10^{16} to 4.68×10^{16} charges/cm². Antibacterial assessment results showed that PET surface immobilized with QAS (PET-PMBAA-QAS) was more effective against MDR *E.coli* as compared to the PET-PMBAA without QAS. Also, PET-PMBAA-100%QAS (19:10 AzH/QAS on surface)

was able to kill CA-MRSA more effectively when amount of active chlorine loading was approximately 800 ppm as compared to lower active chlorine loaded PET-PMBAA-100%QAS.

In third approach, cyclic *N*-chloramine (AzH) and QAS were clicked on PET surface and the complexity of the system was reduced by getting rid of acyclic N-H groups. The PET surface was modified by using propargyl acrylate (PET-PA) instead of MBAA to avoid immobilization of additional N-H groups during surface modification process. The surfaces prepared for testing included PET-PA-70/30 AzH/QAS, 50/50 AzH/QAS and 30/70 AzH/QAS samples. The positive charge density on PET-PA surface was determined using colorimetric method based on 4-(phenylazo) benzoic acid dye. PET-PA-AzH/QAS presented higher active chlorine loading than PET-PA-AzH sample without QAS. Surface charge density of the samples was determined using dye titration method resulting in 6.64×10^{15} charges/cm² on 70/30 AzH/QAS, 2.09×10^{16} on 50/50 AzH/QAS and 2.72×10^{16} on 30/70 AzH/QAS. Moreover, at similar level of active chlorine loading on PET-PA-70/30 AzH/QAS, 50/50 AzH/QAS and 30/70 AzH/QAS surfaces, highest antibacterial activity was observed against MDR *E.coli* (total kill in 10 minutes) when highest amount of positive charge 30/70 AzH/QAS (2.72×10^{16} charges/cm²) was loaded on PET-PA surface. The ratio of cyclic *N*-chloramine and QAC on the surface of 30/70 AzH/QAS sample was found to be 17.2:10 which was determined using QAS charge density and active chlorine loading on this surface.

Overall, our hypothesis is confirmed and we found that the ratio of *N*-chloramine and QAS on amide modified PET for most effective antibacterial activity might not be 1:1. We found that sample loaded with 17.2:10 N-Cl: QAS killed *E.coli* most effectively in 10 minutes. The objectives were achieved in the following sequence: Successful bonding of AzH and QAS was achieved by forming surface interpenetrating network (surface modification method) on PET fabric followed by click reaction with active biocides (AzH & QAS). Also, plasma induced UV photo-polymerization

was conducted as an alternative surface modification method followed by click reaction with AzH and QAS. Introduction of positive charge has contributed to achieving higher active chlorine loading as well as higher antibacterial efficacy on PET surface treated with both cyclic and acyclic *N*-chloramines. Although, the antibacterial efficacy was higher where cyclic *N*-halamines were used in combination with QAS as compared to acyclic *N*-halamine. PET surface treated with cyclic *N*-chloramine and QAS (17.2:10 N-Cl:QAS on surface) where density of positive charge was 2.72×10^{16} charges/cm² achieved 5 log reduction of *E.coli* in 10 min with an active chlorine content of 218 ppm. On contrary, acyclic *N*-chloramine and QAS (19:10 N-Cl:QAS on surface) treated surface demonstrated 5 log reduction of *E.coli* in 60 mins (790 ppm active chlorine) when positive charge density on surface was 8.47×10^{16} charges/cm². Chlorination kinetics results revealed that as the surface charge density on PET-MBAA-QAS reached 4.68×10^{16} charges/cm², 75% of saturated active chlorine loading (477 ppm out of 634 ppm) PET-PMBAA surface was achieved.

Although the contribution of positive charge towards active chlorine loading as well as antibacterial efficacy of modified PET fabric using various ratios has been evaluated, there is a scope of further zooming into the ratios and comparing other possible combinations of AzH and QAS. Also, it is recommended to perform elemental analysis to determine Cl% on fabric in addition to Iodometric titration process. This will help to correlate the amount of active chlorine on surface using two different methods. Significance of this project lies in the finding that a novel class of antibacterial agents can be developed through suitable combination of *N*-chloramine and QAS on modified PET surface. This combination of *N*-chloramine and QAS can result in enhanced conversion of surface bound N-H to N-Cl and faster killing of bacteria.

6 REFERENCE LIST

- (1) Bin, W.; Ho, S.; Park, J.; Hak, S.; Finn, J.; Yoon, S. European Journal of Medicinal Chemistry Discovery of Torezolid as a Novel 5-Hydroxymethyl-Oxazolidinone Antibacterial Agent. *Eur. J. Med. Chem.* **2011**, *46* (4), 1027–1039.
- (2) Vera-cabrera, L.; Gonzalez, E.; Rendon, A.; Ocampo-candiani, J.; Welsh, O.; Velazquez-moreno, V. M.; Choi, S. H.; Molina-torres, C. In Vitro Activities of DA-7157 and DA-7218 against Mycobacterium Tuberculosis and Nocardia Brasiliensis. *Antimicrob. Agents Chemother.* **2006**, *50* (9), 3170–3172.
- (3) Naimi, T. S.; Ledell, K. H.; Como-sabetti, K.; Borchardt, S. M.; Boxrud, D. J.; Johnson, S. K.; Fridkin, S.; Boyle, C. O.; Danila, R. N. Comparison of Community-and Health Care – Associated Staphylococcus Aureus Infection. **2003**, *290* (22).
- (4) Seybold, U.; Kourbatova, E. V.; Johnson, J. G.; Halvosa, S. J.; Wang, Y. F.; King, M. D.; Ray, S. M.; Blumberg, H. M. Emergence of Community-Associated Methicillin- Resistant Staphylococcus Aureus USA300 Genotype as a Major Cause of Health Care – Associated Blood Stream Infections. **2006**, 647–656.
- (5) Klevens, R. M.; Edwards, J. R.; Jr, C. L. R.; Teresa, C.; Gaynes, R. P.; Pollock, D. A.; Cardo, D. M.; Elevens, R. M. Estimating Health Care-Associated Infections and Deaths in U . S . Hospitals , 2002. **2007**, *122* (2), 160–166.
- (6) ROBERT A. WEINSTEIN. Epidemiology and Control of Nosocomial Infections in Adult Intensive Care Units. **1991**.
- (7) Gastmeier, P.; Stamm-balderjahn, S.; Hansen, S.; Zuschneid, I. Where Should One Search When Confronted with Outbreaks of Nosocomial Infection ? **2006**, No. 91, 603–605.
- (8) Arbor, A.; Health, E.; Arbor, A. Epidemiology of Antibiotic-Associated Colitis Isolation Qf Clostridium Difficile from the Hospital Environment. **1981**, *70* (April), 906–908.
- (9) Samore, M. H.; Venkataraman, L.; Degirolami, P. C.; Arbeit, R. D.; Karchmer, A. W. Clinical and Molecular Epidemiology of Sporadic and Clustered Cases of Nosocomial Clostridium Difficile Diarrhea. **1996**, *100* (January).

- (10) Kim, K.; Fekety, R.; Batts, D. H.; Brown, D. Isolation of *Clostridium Difficile* from the Environment and Contacts of Patients with Antibiotic-Associated Colitis. **1981**, *143* (1), 42–50.
- (11) JM, B. Methicillin-Resistant *Staphylococcus Aureus* in Hospitals and Long-Term Care Facilities: Microbiology, Epidemiology, and Preventive Measures. *Infect Control Hosp Epidemiol* **1992**, *13*, 725–737.
- (12) Wilks, S. A.; Michels, H.; Keevil, C. W. The Survival of *Escherichia Coli* O157 on a Range of Metal Surfaces. **2005**, *105*, 445–454.
- (13) Williams, A. P.; Avery, L. M.; Killham, K.; Jones, D. L. Persistence of *Escherichia Coli* O157 on Farm Surfaces under Different Environmental Conditions. **2005**, 1075–1083.
- (14) Rd, M. The Survival and Transfer of Microbial Contamination via Cloths , Hands and Utensils. **1990**, 271–278.
- (15) Panagea, S.; Winstanley, C.; Walshaw, M. J.; Ledson, M. J.; Hart, C. A. Environmental Contamination with an Epidemic Strain of *Pseudomonas Aeruginosa* in a Liverpool Cystic Fibrosis Centre , and Study of Its Survival on Dry Surfaces. **2005**, 102–107.
- (16) Wagenvoort, J. H. T.; Sluijsmans, W.; Penders, R. J. R. Better Environmental Survival of Outbreak vs . Sporadic MRSA Isolates. **2000**, *1*, 231–234.
- (17) Neely, A. N.; Maley, M. P. Survival of Enterococci and Staphylococci on Hospital Fabrics and Plastic. **2000**, *38* (2), 724–726.
- (18) Lankford, M. G.; Collins, S.; Ascp, M. T.; Youngberg, L.; Ascp, M. T. Assessment of Materials Commonly Utilized in Health Care : Implications for Bacterial Survival and Transmission. *Am. J. Infect. Control* **2006**, 258–263.
- (19) Fijan, S.; Turk, S. Š. Hospital Textiles, Are They a Possible Vehicle for Healthcare-Associated Infections? *Int. J. Environ. Res. Public Health* **2012**, *9* (9), 3330–3343.
- (20) Ciston, S.; Lueptow, R. M.; Gray, K. A. Bacterial Attachment on Reactive Ceramic Ultrafiltration Membranes. *J. Memb. Sci.* **2008**, *320*, 101–107.
- (21) Whitehead, K. A.; Verran, J. The Effect of Surface Topography on the Retention of Microorganisms. *Food Bioprod. Process.* **2006**, No. December, 253–259.

- (22) Crick, C. R.; Ismail, S.; Pratten, J.; Parkin, I. P. An Investigation into Bacterial Attachment to an Elastomeric Superhydrophobic Surface Prepared via Aerosol Assisted Deposition. *Thin Solid Films* **2011**, 519 (11), 3722–3727.
- (23) Hermansson, M. The DLVO Theory in Microbial Adhesion. *Colloids Surfaces B Biointerfaces* **14** **1999**, 14, 105–119.
- (24) Jeon, H.; Yi, S.; Oh, S. Preparation and Antibacterial Effects of Ag – SiO₂ Thin Films by Sol – Gel Method. *Biomaterials* **2003**, 24, 4921–4928.
- (25) Lee, D.; Cohen, R. E.; Rubner, M. F. Antibacterial Properties of Ag Nanoparticle Loaded Multilayers and Formation of Magnetically Directed Antibacterial Microparticles. *Langmuir* **2005**, No. 7, 9651–9659.
- (26) Dai, J.; Bruening, M. L. Catalytic Nanoparticles Formed by Reduction of Metal Ions in Multilayered Polyelectrolyte Films. *NANO Lett.* **2002**, 1–5.
- (27) Chen, X.; Cai, K.; Fang, J.; Lai, M.; Li, J.; Hou, Y.; Luo, Z.; Hu, Y.; Tang, L. Dual Action Antibacterial TiO₂ Nanotubes Incorporated with Silver Nanoparticles and Coated with a Quaternary Ammonium Salt (QAS). *Surf. Coatings Technol.* **2013**, 216, 158–165.
- (28) Abbaszadegan, A.; Ghahramani, Y.; Gholami, A.; Hemmateenejad, B.; Dorostkar, S.; Nabavizadeh, M.; Sharghi, H. The Effect of Charge at the Surface of Silver Nanoparticles on Antimicrobial Activity against Gram-Positive and Gram-Negative Bacteria : A Preliminary Study. *J. Nanomater.* **2015**, 2015.
- (29) Vallapa, N.; Wiarachai, O.; Thongchul, N.; Pan, J. Enhancing Antibacterial Activity of Chitosan Surface by Heterogeneous Quaternization. *Carbohydr. Polym.* **2011**, 83 (2), 868–875.
- (30) Tiller, J. C. Antimicrobial Surfaces. In *Bioactive surfaces*; 2010; pp 193–217.
- (31) Li, L.; Pu, T.; Zhanel, G.; Zhao, N.; Ens, W.; Liu, S. New Biocide with Both N -Chloramine and Quaternary Ammonium Moieties Exerts Enhanced Bactericidal Activity. *Adv. Healthc. Mater.* **2012**, 609–620.
- (32) Wang, J.; Lewis, K.; Klivanov, A. M. Immobilized N -Alkylated Polyethylenimine Avidly Kills Bacteria by Rupturing Cell Membranes With No Resistance Developed. *Biotechnol. Bioeng.* **2005**, 0002, 715–722.
- (33) Tiller, J. C.; Liao, C. J.; Lewis, K.; Klivanov, a M. Designing Surfaces That Kill Bacteria on Contact. *Proc. Natl. Acad. Sci. U. S. A.* **2001**, 98 (11), 5981–5985.

- (34) Lin, J.; Qiu, S.; Lewis, K.; Klibanov, A. M. Bactericidal Properties of Flat Surfaces and Nanoparticles Derivatized with Alkylated Polyethylenimines. *Biotechnol. Prog* **2002**, 1082–1086.
- (35) Ignatova, M.; Voccia, S.; Gilbert, B.; Markova, N.; Mercuri, P. S.; Galleni, M.; Lenoir, S.; Cossement, D.; Gouttebaron, R.; Je, C. Synthesis of Copolymer Brushes Endowed with Adhesion to Stainless Steel Surfaces and Antibacterial Properties by Controlled Nitroxide-Mediated Radical Polymerization. *Langmuir* **2004**, No. 13, 10718–10726.
- (36) Lee, S. B.; Koepsel, R. R.; Morley, S. W.; Matyjaszewski, K.; Sun, Y.; Russell, A. J. Permanent, Nonleaching Antibacterial Surfaces, 1. Synthesis by Atom Transfer Radical Polymerization. *Biomacromolecules* **2004**, 5 (3), 877–882.
- (37) Ning, C.; Li, L.; Logsetty, S.; Ghanbar, S.; Guo, M.; Ens, W.; Liu, S. Enhanced Antibacterial Activity of New “composite” Biocides with Both N-Chloramine and Quaternary Ammonium Moieties. *RSC Adv.* **2015**, 5, 93877–93887.
- (38) Gottardi, W.; Nagl, M. N -Chlorotaurine , a Natural Antiseptic with Outstanding Tolerability. **2010**, 21–24.
- (39) Sun, Y.; Sun, G. Novel Refreshable N -Halamine Polymeric Biocides : N-Chlorination of Aromatic Polyamides. **2004**, 5015–5020.
- (40) Sun, G. Durable and Regenerable Antibacterial Finishing of Fabrics: Biocidal Properties. *Text. Chem. Color.* **1998**, 6, 26–30.
- (41) Worley, S. D.; Wu, R.; Kim, J.; Wei, C.; Williams, J. F.; Owens, J. R.; Wander, J. D. A Novel N-Halamine Monomer for Preparing Biocidal Polyurethane Coatings. **2003**, 86 (December), 273–277.
- (42) Ahmed, A. E.-S. I.; Shen, H. M.; Xu, Z. L. Optimizing Halogentaion Conditions of N-Halamine Polymers and Investigating Mode of Bacteria Action. *J. Appl. Polym. Sci.* **2009**, 113 (2), 2404–2412.
- (43) Liu, S.; Sun, G. Durable and Regenerable Biocidal Polymers : Acyclic N -Halamine Cotton Cellulose. *Ind. Eng. Chem.* **2006**, 1, 6477–6482.
- (44) Sun, G. Durable and Regenerable Antibacterial Finishing of Fabrics: Fabric Properties. *Text. Chem. Color.* **1999**, 1, 21–24.
- (45) Sun, G.; Worley, S. D. Products of Chemistry Chemistry of Durable and Regenerable Biocidal Textiles.

2005, 82 (1), 60–64.

- (46) Zhao, N.; Zhanel, G. G.; Liu, S. Regenerability of Antibacterial Activity of Interpenetrating Polymeric N-Halamine and Poly (Ethylene Terephthalate). *J. Appl. Polym. Sci.* **2010**.
- (47) Bisquera, W.; Sumera, F. C. Regenerable Antimicrobial Polyurethane Coating Based on N-Hydroxymethylated Hydantoin. *Philipp. J. Sci.* **2011**, 140 (2), 207–219.
- (48) Sun, Y.; Sun, G. Novel Regenerable N-Halamine Polymeric Biocides. II. Grafting Hydantoin-Containing Monomers onto Cotton Cellulose. *J. Appl. Polym. Sci.* **2001**, 617–624.
- (49) Sun, Y.; Sun, G. Novel Regenerable N-Halamine Polymeric Biocides. III. Grafting Hydantoin-Containing Monomers onto Synthetic Fabrics. *J. Appl. Polym. Sci.* **2001**, 1517–1525.
- (50) Song Liu. Biocidal Acyclic Halamine Polymers: Conversion of Acrylamide-Grafted-Cotton to Acyclic Halamine. *J. Appl. Phys.* **2008**, 113, 3480–3486.
- (51) Liu, S.; Sun, G. New Refreshable N-Halamine Polymeric Biocides: N-Chlorination of Acyclic Amide Grafted Cellulose. *Ind. Eng. Chem. Res.* **2009**, 48 (2), 613–618.
- (52) Sun, G.; Xu, X. J.; Bickett, J. R.; Williams, J. F. Durable and Regenerable Antibacterial Finishing of Fabrics with a New Hydantoin Derivative. *Ind. Eng. Chem. Res.* **2001**, 40 (4), 1016–1021.
- (53) Chen, Z.; Luo, J.; Sun, Y. Biocidal Efficacy, Biofilm-Controlling Function, and Controlled Release Effect of Chloromelamine-Based Bioresponsive Fibrous Materials. *Biomaterials* **2007**, 28 (9), 1597–1609.
- (54) Kou, L.; Liang, J.; Ren, X.; Kocer, H. B.; Worley, S. D.; Broughton, R. M.; Huang, T. S. Novel N-Halamine Silanes. *Colloids Surfaces A Physicochem. Eng. Asp.* **2009**, 345 (1-3), 88–94.
- (55) Ren, X.; Kou, L.; Kocer, H. B.; Zhu, C.; Worley, S. D.; Broughton, R. M.; Huang, T. S. Antimicrobial Coating of an N-Halamine Biocidal Monomer on Cotton Fibers via Admicellar Polymerization. *Colloids Surfaces A Physicochem. Eng. Asp.* **2008**, 317, 711–716.
- (56) Zhao, N.; Liu, S. Thermoplastic Semi-IPN of Polypropylene (PP) and Polymeric N-Halamine for Efficient and Durable Antibacterial Activity. *Eur. Polym. J.* **2011**, 47 (8), 1654–1663.
- (57) Liu, S.; Zhao, N.; Rudenja, S. Surface Interpenetrating Networks of Poly(ethylene Terephthalate) and Polyamides for Effective Biocidal Properties. *Macromol. Chem. Phys.* **2010**, 211, 286–296.

- (58) Angela S. Inácio, A. N. In Vitro Activity of Quaternary Ammonium Surfactants against Streptococcal, Chlamydial, and Gonococcal Infective Agents. *Antimicrob. Agents Chemother.* **2016**, 60 (6), 3323–3332.
- (59) Gozzelino, G.; Tobar, D. E. R.; Chaitiemwong, N.; Hazeleger, W.; Beumer, R. Antibacterial Activity of Reactive Quaternary Ammonium Compounds in Solution and in Nonleachable Coatings. *J. Food Prot.* **2011**, 74 (12), 2107–2112.
- (60) Gozzelino, G.; Lisanti, C.; Beneventi, S. Quaternary Ammonium Monomers for UV Crosslinked Antibacterial Surfaces. *Colloids Surfaces A Physicochem. Eng. Asp.* **2013**, 430, 21–28.
- (61) Isquith, A. J.; Abbott, E. A.; Walters, P. A. Surface-Bonded Antimicrobial Activity of an Organosilicon Quaternary Ammonium Chloride. *Appl. MICROBIOLOGY* **1972**, 24 (6), 859–863.
- (62) Lin, J.; Qiu, S.; Lewis, K.; Klivanov, A. M. Mechanism of Bactericidal and Fungicidal Activities of Textiles Covalently Modified With Alkylated Polyethylenimine. **2003**.
- (63) Huang, J.; Koepsel, R. R.; Murata, H.; Wu, W.; Lee, S. B.; Kowalewski, T.; Russell, A. J.; Matyjaszewski, K. Nonleaching Antibacterial Glass Surfaces via “Grafting onto”: The Effect of the Number of Quaternary Ammonium Groups on Biocidal Activity. *Langmuir* **2008**, 24 (13), 6785–6795.
- (64) Bouloussa, O.; Semetey, V. A New , Simple Approach to Confer Permanent Antimicrobial Properties to Hydroxylated Surfaces by Surface Functionalization W. **2008**, 951–953.
- (65) Gottenbos, B.; Mei, H. C. Van Der; Klatter, F.; Nieuwenhuis, P.; Busscher, H. J. In Vitro and in Vivo Antimicrobial Activity of Covalently Coupled Quaternary Ammonium Silane Coatings on Silicone Rubber. **2002**, 23, 1417–1423.
- (66) Madkour, A. E.; Dabkowski, J. M.; Nu, K.; Tew, G. N. Fast Disinfecting Antimicrobial Surfaces. **2009**, No. 8, 1060–1067.
- (67) Kugler, R. Evidence of a Charge-Density Threshold for Optimum Efficiency of Biocidal Cationic Surfaces. *Microbiology* **2005**, 151 (5), 1341–1348.
- (68) Murata, H.; Koepsel, R. R.; Matyjaszewski, K.; Russell, A. J. Permanent, Non-Leaching Antibacterial surfaces—2: How High Density Cationic Surfaces Kill Bacterial Cells. *Biomaterials* **2007**, 28 (32), 4870–4879.
- (69) Asri, L. A. T. W.; Crismaru, M.; Roest, S.; Chen, Y.; Ivashenko, O.; Rudolf, P.; Tiller, J. C.; Mei, H. C. Van Der; Loontjens, T. J. A.; Busscher, H. J. A Shape-Adaptive , Antibacterial-Coating of Immobilized

Quaternary-Ammonium Compounds Tethered on Hyperbranched Polyurea and Its Mechanism of Action. *Adv. Funct. Mater* **2014**, 346–355.

- (70) Kugler, R.; Bouloussa, O.; Rondelez, F. Evidence of a Charge-Density Threshold for Optimum Efficiency of Biocidal Cationic Surfaces. *Microbiology* **2005**, 151 (5), 1341–1348.
- (71) Xu, W. Z.; Gao, G.; Kadla, J. F. Synthesis of Antibacterial Cellulose Materials Using a “Clickable” Quaternary Ammonium Compound. *Cellulose* **2013**, 20 (3), 1187–1199.
- (72) Li, L.; Zhao, N.; Liu, S. Versatile Surface Biofunctionalization of Poly (Ethylene Terephthalate) by Interpenetrating Polymerization of a Butynyl Monomer Followed by “ Click Chemistry .” *Polymer (Guilf)*. **2012**, 53 (1), 67–78.
- (73) Chen, Z.; Sun, Y. N-Halamine-Based Antimicrobial Additives for Polymers: Preparation, Characterization, and Antimicrobial Activity. *Ind. Eng. Chem. Res.* **2006**, 45 (8), 2634–2640.
- (74) Cao, Z.; Sun, Y. N -Halamine-Based Chitosan : Preparation , Characterization , and Antimicrobial Function. *J. Biomed. Mater. Res.* **2007**, No. April, 99–107.
- (75) Zimmermann, R.; Birkert, O.; Gauglitz, G. Electrosurface Phenomena at Polymer Films for Biosensor Applications. **2003**, 509–514.
- (76) Grancaric, A. M.; Tarbuk, A.; Pusic, T. Electrokinetic Properties of Textile Fabrics. **2005**, 121 (May), 21–24.
- (77) Hiemenz, P. C. and R. R. The Electrical Double Layer and Double-Layer Interactions. *Princ. Colloid Surf. Chem.* **1997**, 499–533.
- (78) Kirby, B. J.; Jr, E. F. H. Review Zeta Potential of Microfluidic Substrates : 2 . Data for Polymers. **2004**, 203–213.
- (79) Kirby, B. J.; Jr, E. F. H. Review Zeta Potential of Microfluidic Substrates : 1 . Theory , Experimental Techniques , and Effects. **2004**, 187–202.
- (80) Gottenbos, B. Antimicrobial Effects of Positively Charged Surfaces on Adhering Gram-Positive and Gram-Negative Bacteria. *J. Antimicrob. Chemother.* **2001**, 48 (1), 7–13.
- (81) Yudovin-farber, I.; Golenser, J.; Beyth, N.; Weiss, E. I.; Domb, A. J. Quaternary Ammonium Polyethyleneimine : Antibacterial Activity. *J. Nanomater.* **2010**, 2010.

- (82) Schaep, J.; Vandecasteele, C. Evaluating the Charge of Nanofiltration Membranes. *J. Membr. Sci.* **188** **2001**, *188* (February), 129–136.
- (83) Bacchi, A.; Costa, M.; Gabriele, B.; Pelizzi, G.; Salerno, G. Efficient and General Synthesis of 5- (Alkoxy carbonyl) Methylene-3-Oxazolines by Palladium-Catalyzed Oxidative Carbonylation of Prop-2-Ynylamides. **2002**, *1999*, 4450–4457.
- (84) Ren, X.; Kocer, H. B.; Kou, L.; Worley, S. D.; Broughton, R. M.; Tzou, Y. M.; Huang, T. S. Antimicrobial Polyester. *J. Appl. Polym. Sci.* **2008**, *2*.
- (85) S. Temmel, W. Kern, T. L. Zeta Potential of Photochemically Modified Polymer Surfaces. *Progr. Colloid Polym. Sci.* **2006**, *132*, 54–61.
- (86) Staude, E.; Lettmann, C.; Mo, D. Permeation and Tangential Flow Streaming Potential Measurements for Electrokinetic Characterization of Track-Etched Microfiltration Membranes. **1999**, *159*, 243–251.
- (87) Callewaert, C.; Maeseneire, E. De; Kerckhof, F.-M.; Verliefde, A. Microbial Odor Profile of Polyester and Cotton Clothes after a Fitness Session. *Appl. Environ. Microbiol.* **2014**, No. August, 6611–6619.
- (88) Childress, A. E.; Elimelech, M. Effect of Solution Chemistry on the Surface Charge of Polymeric Reverse Osmosis and Nanofiltration Membranes. **1996**, *119*, 253–268.
- (89) Walter, W. G.; Schillinger, J. E. Bacterial Survival in Laundered Fabrics. **1975**, *29* (3), 368–373.